



**GEOLOGICAL SURVEY OF CANADA
OPEN FILE 9175**

**Seismic survey results from a buried valley study,
Elora and Guelph, Ontario**

B. Dietiker, A. J.-M. Pugin, H.L. Crow, K.D. Brewer, and H.A.J. Russell



2024

**GEOLOGICAL SURVEY OF CANADA
OPEN FILE 9175**

**Seismic survey results from a buried valley study, Elora and
Guelph, Ontario**

B. Dietiker, A. J.-M. Pugin, H.L. Crow, K.D. Brewer, and H.A.J. Russell

2024

© His Majesty the King in Right of Canada, as represented by the Minister of Natural Resources, 2024

Information contained in this publication or product may be reproduced, in part or in whole, and by any means, for personal or public non-commercial purposes, without charge or further permission, unless otherwise specified.

You are asked to:

- exercise due diligence in ensuring the accuracy of the materials reproduced;
- indicate the complete title of the materials reproduced, and the name of the author organization; and
- indicate that the reproduction is a copy of an official work that is published by Natural Resources Canada (NRCan) and that the reproduction has not been produced in affiliation with, or with the endorsement of, NRCan.

Commercial reproduction and distribution is prohibited except with written permission from NRCan. For more information, contact NRCan at copyright-droitdauteur@nrcan-rncan.gc.ca.

Permanent link: <https://doi.org/10.4095/pd24sxky79>

This publication is available for free download through the NRCan Open Science and Technology Repository (<https://ostrnrcan-dostrncan.canada.ca/>).

Recommended citation

Dietiker, B., Pugin, A. J.-M., Crow, H.L., Brewer, K.D., and Russell, H.A.J., 2024. Seismic survey results from a buried valley study, Elora and Guelph, Ontario; Geological Survey of Canada, Open File 9175 1 .zip file.
<https://doi.org/10.4095/pd24sxky79>

Publications in this series have not been edited; they are released as submitted by the author.

ISSN 2816-7155
ISBN 978-0-660-71353-3
Catalogue No. M183-2/9175E-PDF

SUMMARY

Buried valleys are an important aquifer type within the glaciated landscape of Canada. Complex erosion and fill histories make the definition of a valley's geometry and fill characteristics a challenge. Seismic transects of two previously identified buried valleys were acquired in Ontario at the University of Guelph Arboretum, and in a peri-urban environment south of the town of Elora. A high-resolution, shear (S) and compression (P) wave seismic reflection survey yielded three line-km of data along four transects. This was complemented by a microtremor HVSR (horizontal-to-vertical spectral ratio) survey along the reflection profiles. The goal of the study was to improve resolution of valley geometries and fill characteristics. Additionally, the HVSR method was tested in its efficacy to provide reconnaissance information on the presence of buried valleys with various lithologies and seismic properties associated with contrasts of density.

Both seismic methods successfully delineated the buried valleys despite the challenging geological terrain, which has a number of dense till units and sorted sediments with intervening lower seismic velocities, and consequently, velocity inversions. Three of four seismic reflection transects imaged the buried valleys which are approximately 200 m wide and varied in depth from 30 to 65 m. The valleys have steep asymmetrical sides with a stepwise character at one location. The HVSR survey successfully detected the bedrock surface, and a shallower high resonance unit that correlates with a till unit. Signal intensity was locally diminished by the shallow dense till unit; nevertheless, results were obtained from the deeper valley bottom areas. The HVSR method demonstrated success as a reconnaissance technique where some geological constraint is available. Data, processing information, and final data images are included as appendices to this report.

RÉSUMÉ

Les vallées enfouies constituent un type d'aquifère important dans le paysage glaciaire du Canada. En raison de l'histoire complexe de l'érosion et du remblayage, la définition de la géométrie d'une vallée et des caractéristiques du remblayage peut s'avérer difficile. Des transects sismiques de deux vallées enfouies précédemment identifiées ont été acquis en Ontario à l'Arboretum de l'Université de Guelph et dans un environnement périurbain au sud de la ville d'Elora. Une étude de réflexion sismique à haute résolution, en ondes de cisaillement (S) et compression (P), a permis de recueillir trois kilomètres linéaires de données le long de quatre transects. Cette étude a été complétée par une étude microtremor HVSR (rapport spectral horizontal/vertical) le long des profils de réflexion. L'objectif de l'étude était d'améliorer la résolution des géométries des vallées et des caractéristiques des remblais. En outre, la méthode HVSR a été testée dans son efficacité à fournir des informations de reconnaissance sur la présence de vallées enfouies avec diverses lithologies incorporant des propriétés sismiques variables associées à des contrastes de densité.

Les deux méthodes sismiques ont permis de délimiter avec succès les vallées enfouies en dépit d'un terrain géologique difficile, qui présente un certain nombre d'unités de till denses et de sédiments triés avec des vitesses sismiques intermédiaires plus faibles et, par conséquent, des inversions de vitesse. Trois des quatre transects de sismique réflexion ont permis d'imager les vallées enfouies qui ont une largeur d'environ 200 m et une profondeur variant de 30 à 65 m. Les vallées ont des côtés asymétriques abrupts avec un caractère en escalier à un endroit. Les levés HVSR a permis d'imager la surface du substratum rocheux ainsi qu'une unité de haute résonance moins profonde qui correspond à une unité de till. L'intensité du signal a été localement diminuée par l'unité de till dense et peu profonde ; des résultats ont néanmoins été obtenus dans les zones plus profondes du fond de la vallée. La méthode s'est avérée efficace en tant que technique de reconnaissance lorsque des contraintes géologiques sont disponibles. Dans le cadre de ce rapport, trois annexes contiennent des données, des informations sur le traitement et des images de données finales.

Table of Contents

SUMMARY	i
Table of Contents	ii
1. INTRODUCTION	1
1.1 GEOLOGY OF THE STUDY AREA	2
1.2 THE SEISMIC REFLECTION METHOD	3
1.3 THE HVSR METHOD	4
2. SITE LOCATIONS	4
3. DATA COLLECTION AND PROCESSING	7
3.1 SEISMIC REFLECTION DATA	7
3.2 HVSR DATA	9
4. CALIBRATION BOREHOLE DATA	10
5. RESULTS AND INTERPRETATION	12
5.1 ELORA SEISMIC REFLECTION SECTIONS	12
5.2 ARBORETUM SEISMIC REFLECTION SECTIONS	14
5.3 ELORA HVSR DATA	16
5.4 ARBORETUM HVSR DATA	17
6. DISCUSSION	19
6.1 COMPARISON AND INTEGRATION OF REFLECTION SEISMIC AND HVSR	19
6.2 SUBJECTIVITY OF INTERPRETATIONS	21
6.3 DIFFERENCES BETWEEN REFLECTION IMAGES AND RESISTIVITY MODELS	23
7. CONCLUSION	24
8. ACKNOWLEDGMENTS	24
9. REFERENCES	25
Appendix 1: DATA PROCESSING	29
A1.1 SEISMIC REFLECTION DATA	29
A1.1.1 Processing	29
A1.1.2 Depth conversion	31
A1.2 HVSR DATA	33
A1.2.1 HVSR method explained	33
A1.2.2 Depth Conversion	35
Appendix 2: SEISMIC PROFILES IN LARGE FORMAT	36
Appendix 3: SEISMIC DATA IN SEG-Y-FORMAT	36
Appendix 4: RAW HVSR DATA	37

1. INTRODUCTION

Buried valleys are an important aquifer type in Canada and may refer to bedrock interface hosted valleys and sediment hosted valleys that have been infilled and covered with sediment (e.g., Russell et al., 2004; Sharpe et al., 2013). A suite of valley types has been recognized in southern Ontario, and they have been the focus of interest since the late 19th century when Spencer (1881) first identified the Laurentian channel. Subsequently a host of valley locations have been investigated (e.g., Greenhouse and Karrow, 1994; Pullan et al., 2004; Russell et al., 2007; Steelman et al., 2018; Bajc et al., 2018; Sharpe et al., 2018; Gerber et al., 2018) and most recently mapped by Gao (2011). Based on this mapping as well as valley distribution, size and depth, bedrock valleys in southern Ontario have been assigned to one of three groups: i) escarpment troughs, ii) escarpment re-entrants, and iii) cuesta gorges (Russell et al., 2007). Valleys have been mapped on the basis of water well records, drilling and geophysics. Geophysical methods provide some of the most complete and reliable information on the various types of buried valleys investigated. Geophysical approaches used to map buried valleys in southern Ontario include seismic refraction, electrical-resistivity, gravity (Greenhouse and Karrow, 1994; Steelman et al., 2018), seismic reflection (Pullan et al., 2004; Pugin et al., 1998), and more recently, airborne electromagnetic techniques (Conway-White et al., 2022).

Initial geophysical investigation of the Elora buried valley was completed by Greenhouse and Karrow (1994). Recently the valley orientation and geometry have been mapped in greater detail by airborne geophysical surveys in Elora (magnetic, electromagnetic), and surface geophysical transects i.e., seismic refraction, electrical resistivity (Steeleman et al., 2018; Conway-White et al., 2022, 2023), and borehole coring/geophysical logging in Elora and Guelph (Steeleman et al., 2018).

To augment the work completed to date in the Elora and Guelph areas, data collection using two seismic techniques was completed over the buried bedrock valleys. This work is a contribution to the collaboration between the Morwick G360 Groundwater Research Institute (MG360) and the Geological Survey of Canada (GSC) to enhance knowledge and datasets at our respective borehole calibration facilities. This report documents the acquisition and processing of high-resolution shear (S)- and compressional (P)-wave seismic reflection data and the microtremor Horizontal-to-Vertical Spectral Ratio (HVSr) method. HVSr data were collected along the seismic reflection profiles to test the method's efficacy in providing reconnaissance information over buried valleys, improve the interpretation of seismic-reflection data, and to test the method's performance in complex geological settings.

Cover photograph: Aug. 2022, Microvibe and landstreamer collecting seismic reflection data along the Elora Trail. Photograph by H. Crow. NRCan photo 2023-299.

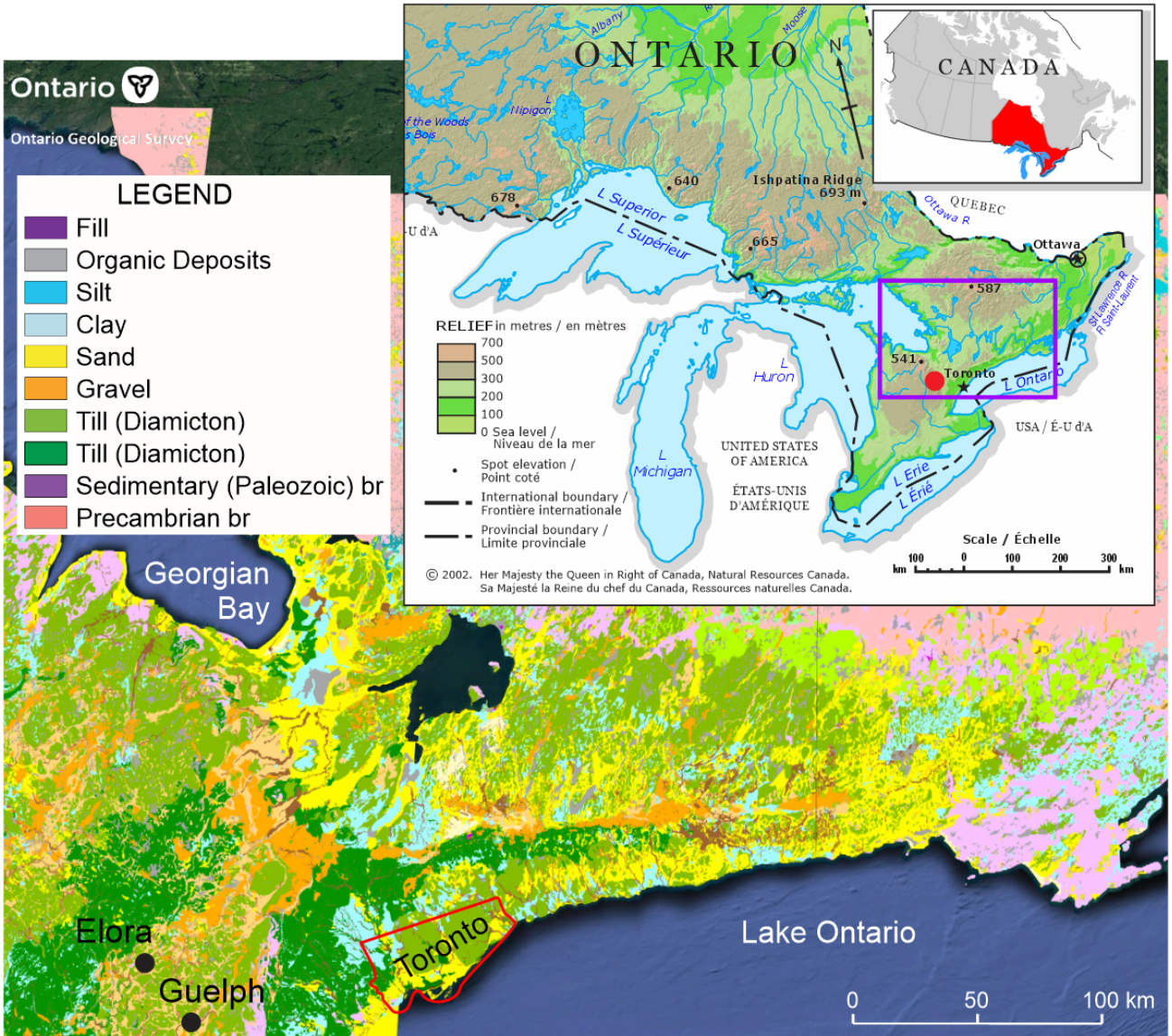


Figure 1. Surficial geology (modified from Ontario, Ministry of Mines, 2012) with study areas indicated. Glacial sediments such as diamicton, gravel and sand, predominate in Southern Ontario.

1.1 GEOLOGY OF THE STUDY AREA

The study area is located atop the Niagara Cuesta and is underlain by Silurian Carbonates of the Lockport Group. The subcropping bedrock unit beneath the Guelph seismic profiles is the Eramosa Formation. Beneath the Elora profiles are variably the Wellington and Hanlon Members of the Guelph Formation on the valley flanks, and the Ancaster Member of the Goat Island Formation in the valley base (see Brunton and Brintnell, 2020). Erosional development within the limestone-dolostone may be the result of successive events of subaerial and subglacial erosion and dissolution (Cole et al., 2009)

Sediments of the Pleistocene epoch document a complex pattern of glacial advances and retreats, as evidenced by deposition and erosion (Barnett, 1992; Fig. 1). The glacial geology of the area has been mapped by Karrow (1968) who identified a succession of till units, and sand and gravel deposits in the area. The till units consist of preCatfish till (Conway-White et al., 2022), Catfish Creek Till, an

intermediate till (Maryhill Till) and younger tills (Port Stanley Till), depending on the location. The Guelph drumlin field is a notable surface expression mapped as Wentworth Till (Karrow 1968) but reassigned by Karrow (1974) to Port Stanley Till. Extensive sand and gravel deposits occur in outwash plains, kames, eskers, in spillway terraces along the Grand River, and amongst the Guelph Drumlin field. Buried valleys within the area have heterogeneous fills of mud, sand, gravel, and till (Greenhouse and Karrow, 1994; Steelman et al., 2018; Conway-White et al., 2022).

Within buried valleys (Elora), waterlain sediment and preCatfish Creek Till have been interpreted by Greenhouse and Karrow (1994) and Conway-White et al. (2022). Catfish Creek Till was the oldest till mapped in the area by Karrow (1968) and is a sandy silt till. It is very dense, and in sections up to 12 m thick. It has been mapped as infilling buried valleys with thickness of 30 m (Steeleman et al., 2018). In water well drillers' logs it is commonly referred to as hardpan (Karrow, 1987). In the Waterloo Moraine area, it has S- and P-wave velocities exceeding 650 and 2500 m/s, respectively (Bajc et al., 2014; Crow et al., 2018). A clayey silt to clay till (the Maryhill Till) that is < 10 m thick occurs in an intermediate stratigraphic position between underlying Catfish Creek and younger Port Stanley Till (Karrow 1974). Port Stanley Till is a sandy to silty sand till with a buff colour; it may be stoney and ranges in thickness from a few metres to 30 m in drumlins (Karrow 1968).

1.2 THE SEISMIC REFLECTION METHOD

Seismic reflection methods have been used most extensively in exploration for oil, gas, and minerals in crustal structures but is also applied in (hydro)geological, archeological, and geotechnical investigations of the near surface (less than a few hundred meters depth). Principles of seismology, comparable to optical-ray theory, consider seismic waves generated by a source (a seismic vibrator in this study) which are reflected and refracted at layer boundaries in the subsurface. The seismic waves which return to the surface are registered by movement sensors called geophones. The recorded raw data are processed to yield reflection profiles. A smooth boundary between soft and hard material creates strong reflections, whereas seismic waves traveling through inhomogeneous materials are affected by scattering and diffractions and produce weak and chaotic reflections.

The main goal of these high-resolution seismic reflection transects was to image the buried valleys' size and shape in greater detail, and to improve the definition of the valley sediment architecture. Using the combination of S- and P-wave transects reveals information about subsurface materials. While P-waves travel much faster than S-waves, they have larger wavelengths and consequently image thicker layers. The resolution of layers thinner than a quarter of the wavelength is difficult to impossible.

P-waves are sensitive to the fluids in the pore space and therefore the first strong reflection is usually related to the water table (Figure A1, see Appendix A1). It is visible in many of the P-wave (depth) sections. S-waves propagate only in solid materials and hence are not influenced by fluids in the pore space. Because of their shorter wavelength, they scatter more easily in heterogeneous materials (such as till or gravel), providing chaotic, low amplitude reflections. This can be observed in parts of the valley fill of Elora.

Seismic reflection interpretations depend mainly on reflection strength (amplitudes) and continuity. Continuous reflections are used to trace a layer boundary. Areas of chaotic reflections delineate regions of heterogeneity, and low amplitudes stem from areas of low density and low velocity contrasts.

1.3 THE HVSR METHOD

The microtremor Horizontal-to-Vertical Spectral Ratio (HVSR) method is used for passive-seismic site characterizations. In recent years, studies have used the method to obtain bedrock or firm-ground depth estimates and as such have become useful for groundwater investigations. The frequency spectrum of these recorded minuscule ground motions is affected by the sediment thickness and velocity structure of the measurement site. The diagnostic characteristic of the processed dataset is an amplification peak, i.e. a resonance at a fundamental frequency. The fundamental frequency is related to the average shear-wave velocity and the total sediment thickness which is usually interpreted to equal the bedrock depth. More information can be found in Appendix A1.2.

Good HVSR results are obtained in areas with a simple geological succession where shear-wave velocities steadily increase with depth, and where a strong contrast exists between sediments and bedrock (e.g., glacial marine/lacustrine environments over till or rock). In areas of complex glacial history where layer(s) of lower S-wave velocity underlie higher velocity layer(s) (e.g., multiple till layers), contrasts and inversions can negatively impact HVSR results. To test the performance in these complex geological settings, HVSR data were collected and analyzed. Additionally, the efficacy in providing reconnaissance information over buried valleys was explored by siting the measurements along the seismic reflection profiles.

2. SITE LOCATIONS

Detailed seismic reflection profiles of two previously identified buried valleys were acquired at (1) the University of Guelph Arboretum (see Steelman et al. 2018), and (2) a peri-urban environment south of the town of Elora in Central Wellington Township, ON (see Conway-White, 2020; Conway-White et al., 2022). Profiles were acquired along a total of four alignments in Guelph and Elora (Figure 2) between Aug 23 and Aug 28, 2022 by participants from the Geological Survey of Canada (GSC), the Morwick G360 Groundwater Research Institute (MG360), and the University of Waterloo. S- and P-wave data were acquired in separate passes (Table 1).

The Guelph Arboretum is the site of MG360's Fractured Rock Observatory (FRO), a series of ten bedrock boreholes drilled for ongoing multidisciplinary groundwater research (Steelman et al., 2018; Maldaner et al., 2019; Munn et al., 2020). The boreholes intersect approximately 12 – 15 m of Quaternary sediment before entering bedrock and are drilled on the flank of a buried bedrock valley. One of the seismic profile alignments passed by the FRO boreholes to investigate shallow subsurface conditions, sediment architecture, and groundwater pathways to support ongoing research at the FRO (Figure 2). Line "Arbo1" was terminated at the intersection of College Ave E and did not intersect the axis of the buried valley, but the valley was crossed on Arbo 2. The Elora valley was intersected on both Elora alignments, which were selected to pass by boreholes cored and logged by MG360 (Conway-White, 2020; Steelman et al., 2018).

Table 1. Details (with coordinates in UTM NAD83, zone 17) of the seismic data acquisition in Guelph and Elora, 2022.

Name	Location	start		end		length (m)	# HVSr sites
		Easting	Northing	Easting	Northing		
Elora1_S	Cottontail Trail, South of Elora	548345	4836933	548810	4836467	658	43
Elora1_P	Cottontail Trail, South of Elora	548348	4836929	548811	4836466	654	
Elora2_S	Road 6N, East of Elora	546423	4833917	545768	4834566	922	28
Elora2_P	Road 6N, East of Elora	546463	4833878	545776	4834559	967	
Arbo1_S	Arboretum, North of College Ave E	562967	4821297	562940	4821672	376	19
Arbo1_P	Arboretum, North of College Ave E	562916	4821643	562979	4821269	379	
Arbo2_S	Arboretum, South of College Ave E	563371	4821381	563253	4820883	512	23
Arbo2_P	Arboretum, South of College Ave E	563259	4820892	563447	4821229	387	

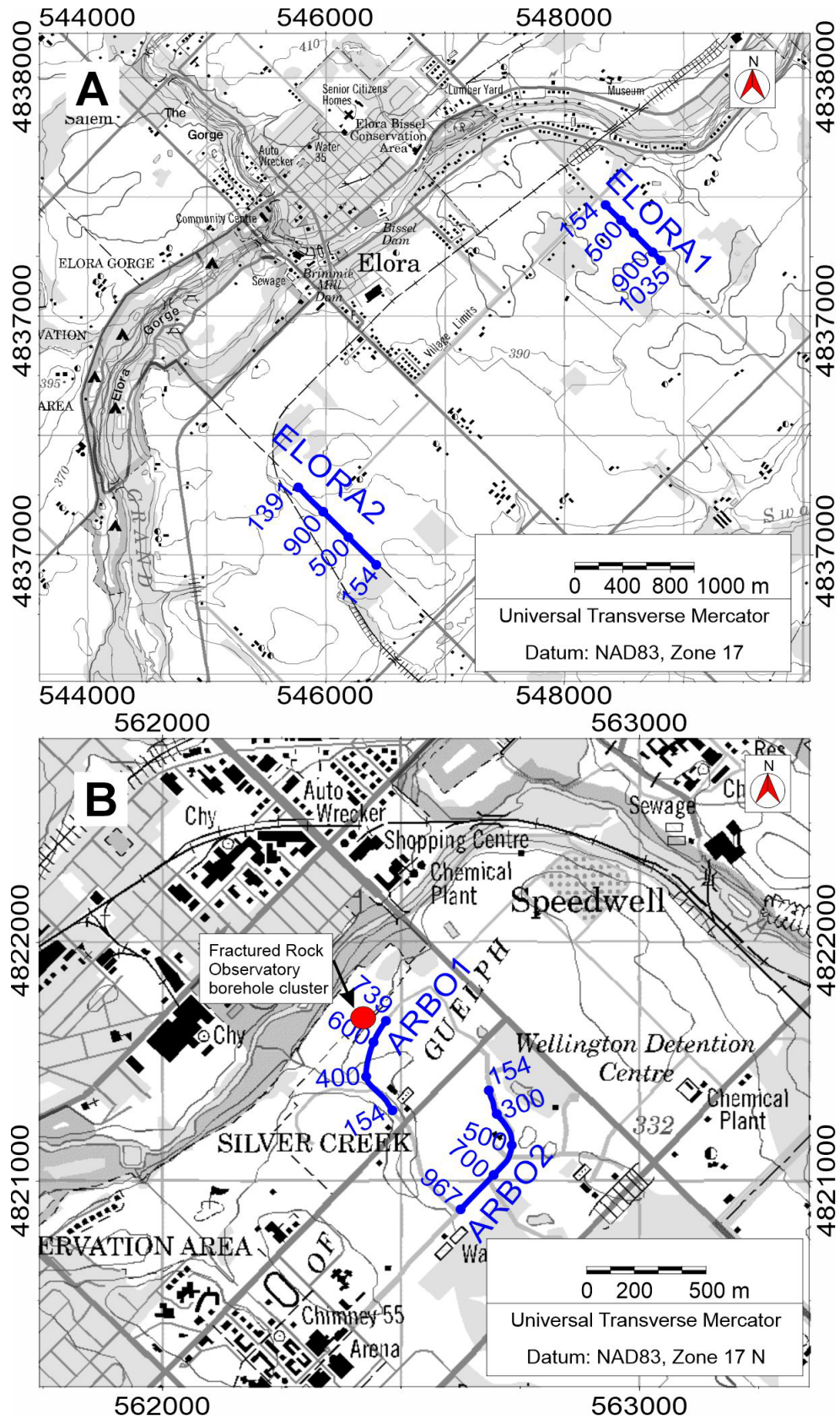


Figure 2. Location of the seismic profiles in the Elora area (A) and the University of Guelph Arboretum (B). Numbers indicate common midpoint (CMP) trace numbers. Elora1 and Elora2 are referred to as the Road (6N) and Trail transects, respectively, in Conway-White (2022). Red dot shows approximate position of the Fractured Rock Observatory borehole cluster on the Guelph Arboretum.

3. DATA COLLECTION AND PROCESSING

3.1 SEISMIC REFLECTION DATA

Seismic energy for the survey was generated by a vibratory source, a GSC invention called the Microvibe (Brewer et. al., 2013). The Microvibe delivers frequency sweeps from 5 to 800 Hz, with up to 2000 W of output power. Horizontal-transverse excitations (perpendicular to the profile) are used to create S-wave vibrations, and vertical excitations create the P-wave vibrations. Each sweep, linearly increasing in frequency, lasted for 9 seconds, with a recording time of 10 seconds starting at the beginning of the sweep. P- and S-wave profiles were acquired in separate passes using source parameters listed in Table 2. Reflected vibrations were recorded with a landstreamer consisting of 48 three-kg metal sleds towed 1.5 m behind the source, with 1.5 m separation between sleds (Table 2). Each sled carries three 28 Hz omnidirectional geophones triaxially mounted: vertical (V), in-line horizontal (H1) and transverse horizontal (H2) (Figure 3). Source locations were determined with real-time differential-GPS measurements.

Table 2. Seismic data-acquisition parameters for Guelph and Elora surveys, 2022.

Line	Sweep			Recording	Geometry
	orientation	start freq (Hz)	end freq (Hz)	interval (ms)	shot spacing (m)
Elora1_P (Trail)	V	20	450	0.5	3
Elora1_S (Trail)	H2	20	250	1	3
Elora2_P (Road 6N)	V	20	450	0.5	3
Elora2_S (Road 6N)	H2	20	250	1	3
Arbo1_P	V	20	450	0.5	1.5
Arbo1_S	H2	20	350	1	1.5
Arbo2_P	V	20	450	0.5	3
Arbo2_S	H2	20	350 / 220	1	1.5
orientation	V	= vertical	H2	= perpendicular to profile	
geophones	28 Hz	48 channels	1.5 m	distance	

The processing steps of seismic reflection data are described in detail in Appendix 1.1. A summary of processing steps and outputs is provided in Table 3 for the reflection profiles. The resulting profiles are discussed in Section 5.



Figure 3. Microvibe and seismic landstreamer array being towed along the Elora Trail (Elora1). Photograph by H. Crow. NRCan photo 2023-299.

Table 3. Processing steps applied to Guelph and Elora seismic reflection datasets and resulting profiles.

Initial processing (all data)		Result
Format conversion, SEG2 to KGS SEGY		
Pilot trace based cross-correlation		
Separation of V, H1, H2 components		
Frequency filter		
Applying of geometry		
Statics calculation (refraction analysis)		
Common midpoint (CMP) sorting		
P-Wave V component (250 ms)	S-Wave H2 component (1000 ms)	
Refraction static correction	fk- and bandpass filter	
fk- and bandpass filter	Scaling (trace normalization)	
Scaling (trace normalization)	Top mute (P-, surface waves)	
Bottom mute (S-, surface waves)		
Velocity semblance analysis	Velocity semblance analysis	Velocity section
NMO corrections	NMO corrections	
Stacking	Stacking	
Topography correction	Topography correction	time section
Time to depth conversion	Time to depth conversion	depth section

3.2 HVSR DATA

A total of 113 passive-seismic microtremor measurements were recorded along the four profiles at a station spacing of 10 m to 20 m (see Table 1). The microtremor Horizontal-to-Vertical Spectral Ratio (HVSR) method utilizes a three-component (two horizontal and one vertical) high-sensitivity seismometer to record ambient seismic vibrations. In this study a small, digital instrument (Tromino® by Moho Science and Technology, Castellaro et al., 2005; Figure 4) was used to record in the frequency range of 0.1 to 30 Hz. Processing steps for a single station HVSR measurement result in a curve of H/V amplitudes as a function of frequency (Table 4). Depth conversion is based on velocities from the semblance analysis of seismic reflections and adjusted for an optimal fit (see Appendix A1.2).

The raw data from ambient 3-component microseismic ground motion records (30-minute time series in m/s at 128 Hz sampling frequency) are available as mini seed files (Ahern et al., 2012) in Appendix A4. There is a file for each of the 113 stations. The filenames include station name, UTM coordinates and instrument azimuth measured during set-up.

Table 4. Processing steps applied to a single station HVSR record.

Processing	Result
Format conversion to mini seed	
Windowing into 60s long time segments	
Fourier Transform	
H/V calculation	H/V amplitudes as a function of frequency
Removing of transient noise	
max(H/V)	Frequencies of maxima (global f_0 and local)
Frequency to depth conversion	Amplitudes, azimuths and significances as a function of depth



Figure 4. HVSR data collection in the Arboretum. Photograph by H. Crow. NRCan photo 2023-300.

4. CALIBRATION BOREHOLE DATA

Borehole information is crucial not only for depth conversion of the time-domain seismic profiles, but also for the lithological interpretation and verification of seismic reflection horizons. Table 5 lists the boreholes which were used in the analyses and interpretation of each profile. The detailed Quaternary stratigraphy of the boreholes in bold are shown on Figure 5.

Table 5. List of boreholes used to support seismic calibration (Locations in NAD83, Zone 17). Boreholes listed in bold are shown in Figure 5.

name	Easting	Northing	elevation	seismic profile	reference
ELR2-QA	548589	4836701	403	Elora1	Data courtesy of MG360, University of Guelph
ELR2-R1	548576	4836711	403	Elora1	Data courtesy of MG360, University of Guelph
ELR2-R2	548403	4836888	405	Elora1	Data courtesy of MG360, University of Guelph
UW2	548512	4836771	402	Elora1	Greenhouse and Karrow, 1994; Conway-White, 2020
ELR1-QB	546178	4834172	378	Elora2	Data courtesy of MG360, University of Guelph
ELR1-R1	546171	4834179	378	Elora2	Data courtesy of MG360, University of Guelph
ELR1-R2	546058	4834293	379	Elora2	Data courtesy of MG360, University of Guelph
GDC-10A	562876	4821595	328	Arbo1	Steelman et al, 2018

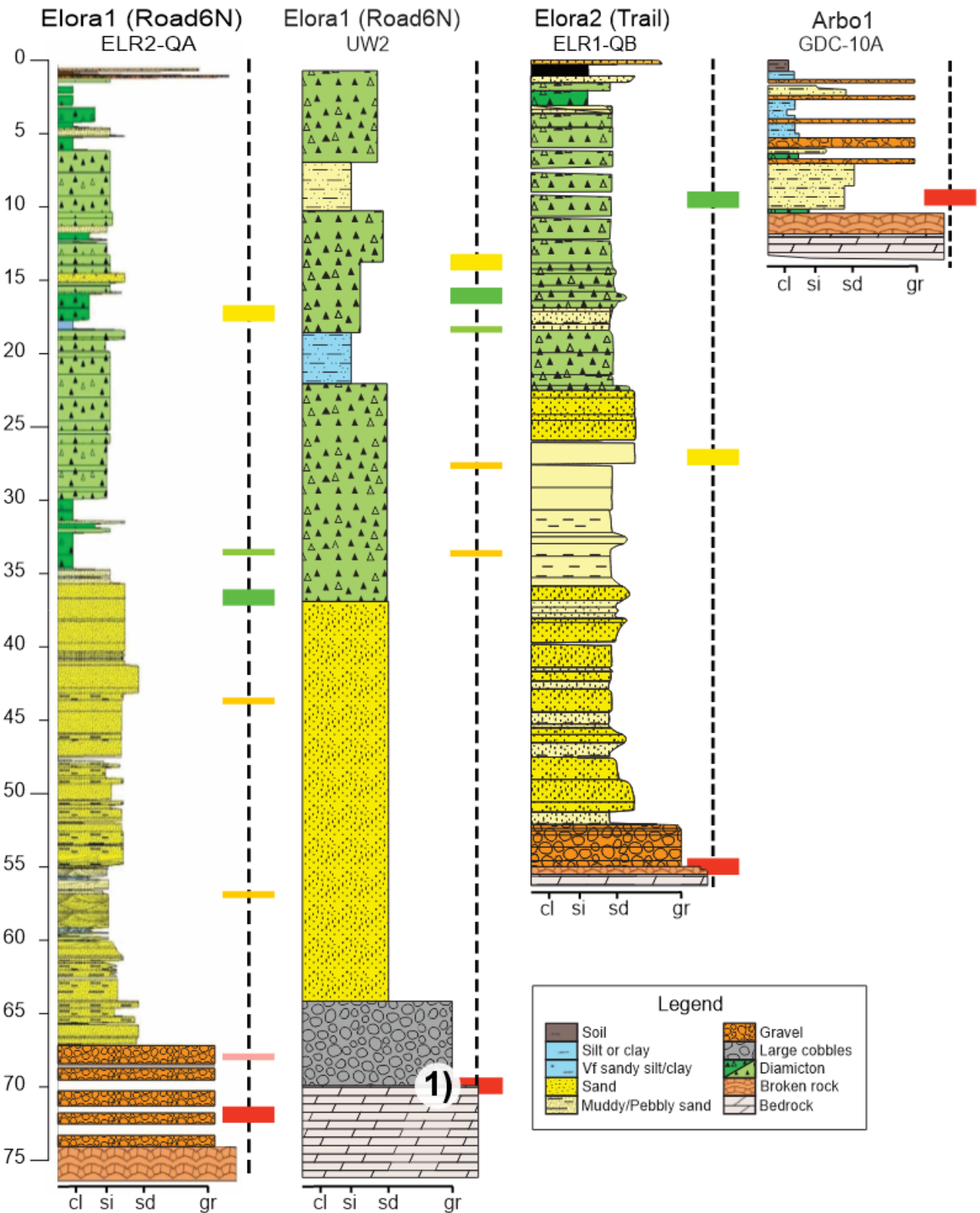


Figure 5. Borehole lithology from verification wells with interpreted horizons as shown on the seismic reflection profiles. 1) Note that the exact top of rock at UW2 could not be confirmed (noted by Hilton, 1978). References are provided in Table 5.

5. RESULTS AND INTERPRETATION

The seismic reflection section data are presented in Appendix A2 as large-format PDF files which can be enlarged for greater detail. An example is shown in Figure 6 and the elements of the figure are as follows:

- Two columns: shear-wave data on the left and P-wave data on the right
- Top row: time-domain sections
- Second row: interpreted depth sections
- Third row: NMO or stacking velocities
- Fourth row: interpretations
- Bottom left: depth-converted H/V amplitudes as green lines, with black lines marking locations
- Bottom right: map indicating profile with common midpoint (CMP) numbers

Distance along the profile as well as trace numbers labelled as CMP are shown on top of every section. Note that the vertical exaggeration for all depth sections is 1.5x (VE=1.5).

In this study glacial sediments create a highly variable velocity structure because of several interspersed high-velocity till layers, including a high-velocity till at surface. Velocity reversals with depth, steep valley walls, and rapid density and velocity changes (vertically and laterally) create challenges for interpretation.

5.1 ELORA SEISMIC REFLECTION SECTIONS

On the Elora S- and P-wave seismic reflection profiles, the continuous high-amplitude reflections are interpreted as the deeply eroded (30 to 65 m) and shallow (≤ 30 m) bedrock surfaces (Figure 6). The P-wave data returns are stronger and of a more coherent continuous signal character than the S-wave data. This is particularly notable at depth along the bottom of the buried valley.

On both Elora transects (Figure 7, Table 6) high-amplitude reflections can be identified, which are created by a high impedance contrast, like gravel, diamicton or bedrock. A layer of diamicton might be misinterpreted as bedrock, leading to an underestimation of depth to bedrock. The sides of the buried valley do not create recordable reflections where they are too steeply inclined (more than 45°) and are therefore indicated by a dashed line on the figures. The interpreter is left to infer the sides from truncated or disrupted reflections. The two buried valleys have similar widths of approximately 200 m with asymmetrical cross-sections. The valley depths differ between the two transects by approximately 35 m with depths of 65 and 30 m along Elora 1 and 2 transects, respectively. The bedrock interpretation for the basal strong reflection is confirmed by the depth to bedrock reported in the boreholes (see Figure 5).

The sediment succession above bedrock has a number of continuous medium-amplitude seismic reflection patterns (highlighted as coloured horizons in Figure 7). The fill of the buried valley is not homogeneous and is best described by a centre fill and an edge fill, as discriminated from a difference in reflection pattern. This is observable on both profiles but more obvious on Elora2. The centre fill has medium-strength, discontinuous reflections, whereas the edge fill consists of continuous high-amplitude reflections that correspond to various sand layers observed in the cored well near the southern margin (ELR1-QB in Figure 7). At the northwestern valley edge of the Elora2 profile, the reflection package is of very high amplitudes filling the whole valley thickness (~ 20 m) with reflections of very similar wavelengths (~ 3.5 m). These reflections are reverberations (ringing) caused by the strong impedance

contrast between diamicton (likely Catfish Creek Till) and the underlying sand units. The discontinuous character and lack of strong reflections point to diamicton filling the central part (CMP 670 to 800, below the green horizon). At Elora1, similar observations can be made with more continuous reflections south of borehole ELR2-R1. It is possible that the central part of the valley fill was first removed by an erosion event, then subsequently refilled. There is no drillhole information available to confirm this hypothesis. However, slight variations in resistivity values (Figure 7 of Conway-White et al., 2022) are consistent with this interpretation.

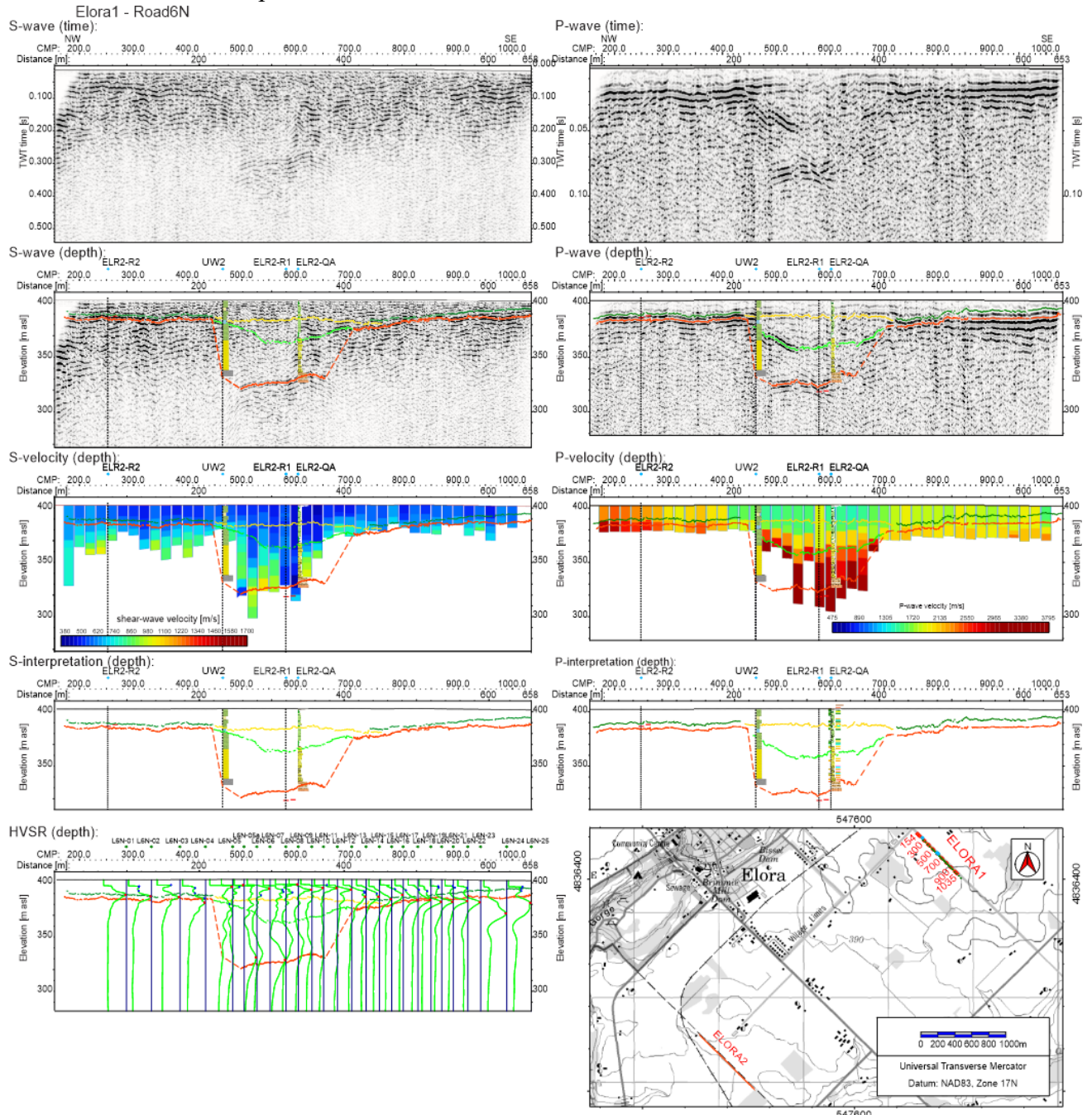


Figure 6. Example of the seismic reflection data (Elora1 – Road6N); large scale (100 x 100 cm) layouts are provided in Appendix A2. Left: S-wave data; right: P-wave data. Top to bottom: Time domain sections, interpreted depth domain sections, NMO velocities, interpretations, HVSR profile and location map. All depth sections are shown with a vertical exaggeration of 1.5.

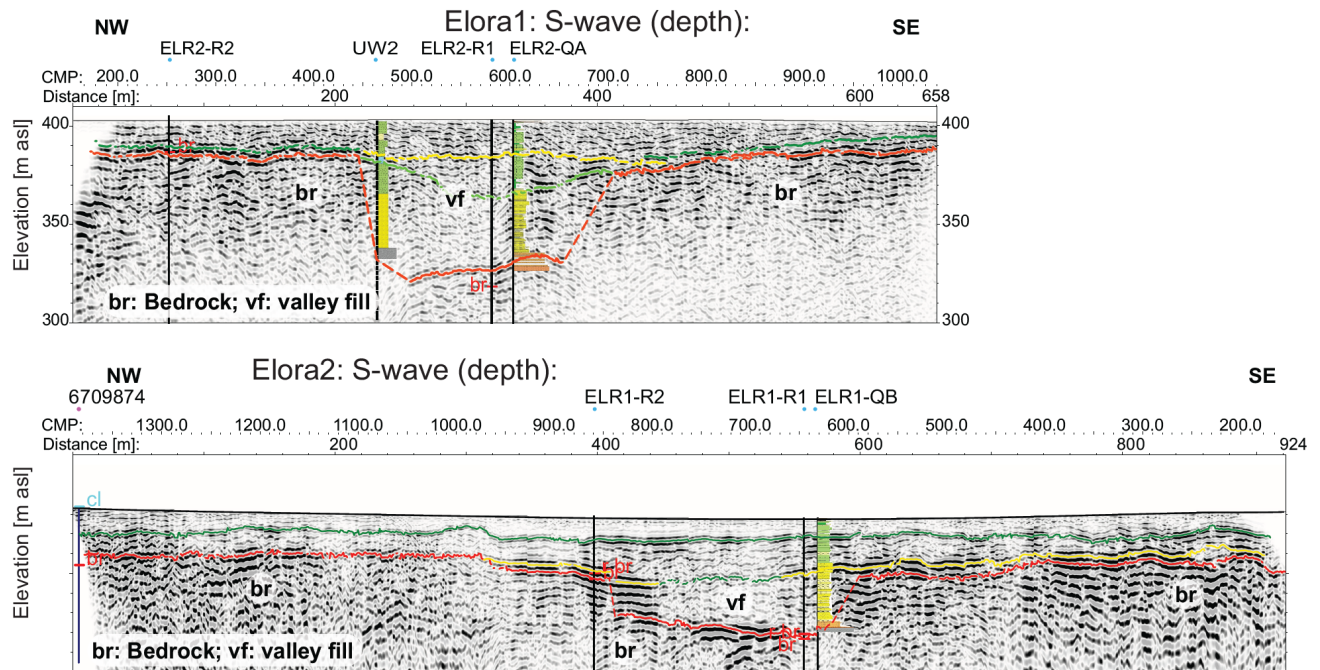


Figure 7. Shear-wave seismic depth section for both Elora profiles with interpretations and borehole control (VE=1.5).

5.2 ARBORETUM SEISMIC REFLECTION SECTIONS

Of the two profiles collected at the Guelph Arboretum, a buried valley was intersected only on the Arbo2 profile (Figure 8, Table 6). Existing borehole and resistivity profile data suggest the valley axis extends under College Ave E beyond the start of Arbo1. The long landstreamer array could not be towed across the road because of high traffic volumes. At Arbo1, dry and heterogeneous surface materials make seismic interpretation challenging. Nevertheless, it would appear that sediment layers form a ~10 m deep depression between CMP 300 and 400 of Arbo1, at the low point of the topographical surface. The location of the Fractured Rock Observatory borehole cluster is shown by the GDC-10 borehole profile near CMP 600.

At Arbo2, the buried valley is interpreted to be 190 m wide with a 50 m deep and 100 m wide thalweg and a shallower southern shoulder of 30 m depth and 90 m width. The northern edge is steep, and the southern edge forms a step inclined SW margin (Figure 8). The seismic contrast between fill material and bedrock is small, hence lowering the reflection amplitudes and making the valley bottom reflections harder to interpret. The low contrast indicates that the infill material is dense, most likely a till. Nearby borehole data supports this interpretation (Steelman et al., 2018).

Much of the valley fill seems chaotic without definable layers. However, shallow potentially erosional layers were interpreted as south-west dipping truncation surfaces (Figure 8). However, the interpretation of these shallowest reflections is complicated by the interference of reflected waves with surface waves, a situation requiring careful interpretation.

Table 6: Summary comparison and highlights of seismic reflection interpretations. Note that “burial” refers to the sediments above the valley.

Highlights	Elora1	Elora2	Arbo1	Arbo2
valley width (m)	~200	~200	NA	190 m total; shoulder 90 m; thalweg 100 m
valley depth, infill thickness (m)	30	30	NA	30-50
burial thickness (m)	15	25	10 - 15	10 - 15
burial reflection character	- medium strength - chaotic	- transparent to medium strength - continuous	continuous, truncations, dipping	
valley fill reflections, centre	- discontinuous - chaotic - low amplitude	- discontinuous - chaotic - low amplitude	NA	chaotic
valley fill reflections, edges	- medium strength - continuous	- high-amplitude reverberations - medium strength - continuous	NA	NA
bedrock reflections, shallow	- high amplitude - continuous	- medium to high amplitude - continuous	- medium to high amplitude - partially discontinuous	- low to medium amplitude - continuous
bedrock reflections, deep	- medium amplitude - continuous	- high amplitude - structured	NA	- medium amplitude - discontinuous

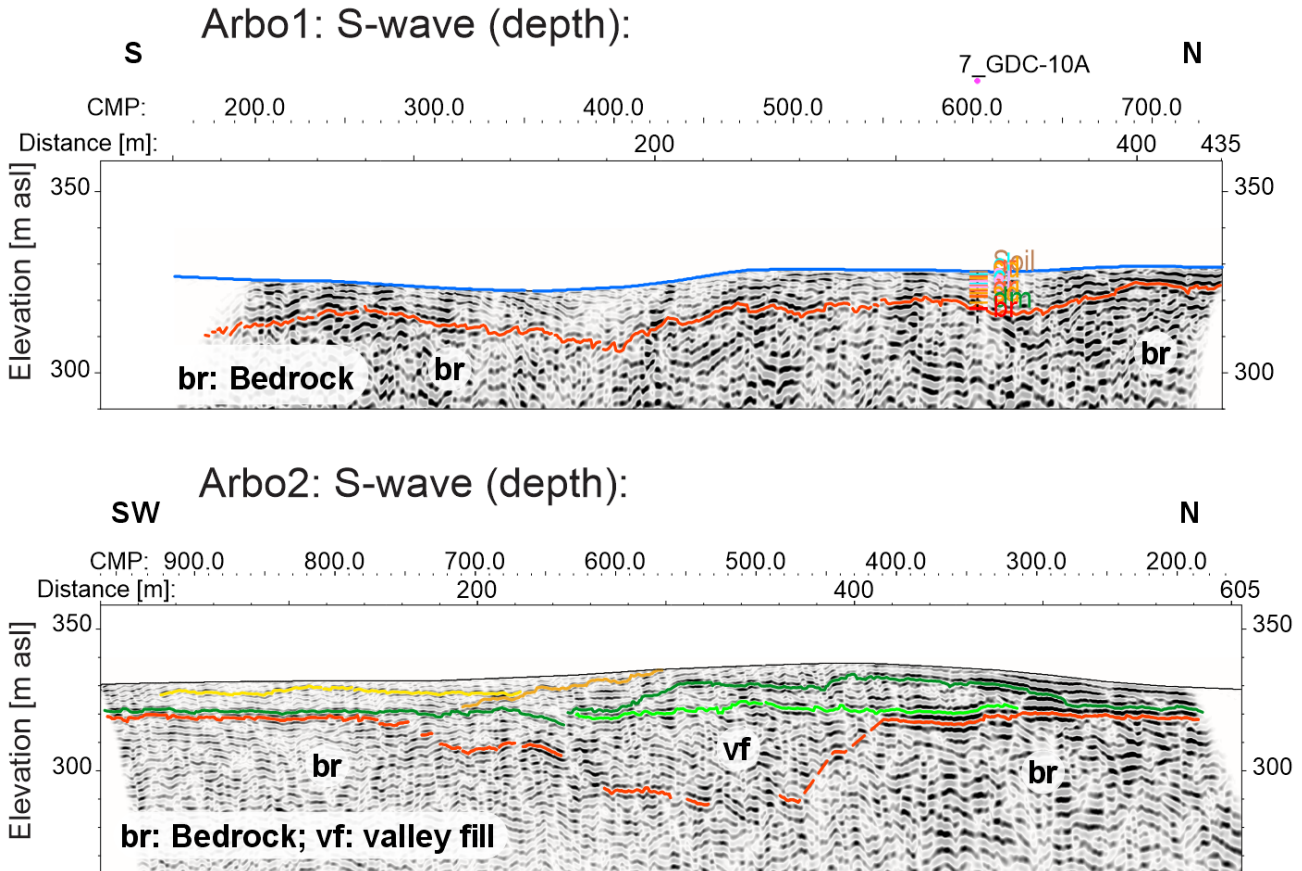


Figure 8. Interpreted shear-wave seismic reflection profiles at the Guelph Arboretum (VE=1.5). Lithological horizon tops of bedrock, sand, till are highlighted as red, yellow, dark and light green respectively.

5.3 ELORA HVSR DATA

Processed HVSR data are presented as depth converted HVSR amplitudes (refer to Appendix A1.2 for a description of the process). At the bottom left of Figure 6 and all figures of Appendix A2, the H/V ratio (green) for each station is displayed on the left of the station location (vertical line), such that the maximum aligns with the location marker. Maxima are highlighted by red dots/crosses (absolute maximum) and blue dots/x's (local maxima).

Depths with increased H/V ratios, established by local and global H/V maxima, are interpreted to be stiff layers, for example till and/or bedrock. The deepest peaks are connected as likely bedrock surface and as delineation of the buried valley. The connections are linked to create a smooth valley outline, as the method estimates trends, without expectation of detail.

For both HVSR profiles at Elora1 and Elora2 (Figure 9) there are some stations with two distinct peaks, a shallow peak at 10 to 20 m depth and a peak at depth greater than 40 m. At Elora1 the shallow peaks increase in strength from a minimum in the northwest to a maximum in the southeast. South of CMP 700, on Elora1 the peaks expand and merge with the deeper peaks. Between CMP 500 and 650 the deeper peaks are weaker but form recognizable maxima which outline the buried valley.

The very high H/V peaks in the center of Elora2 are most evident, outlining a shallow but very stiff layer (Figure 9, bottom). At Elora2 the shallow peaks mask the underlying structure to some extent, but the buried valley feature is still indicated by the deep local H/V maxima (CMP 600 to 950 deeper than 70 m).

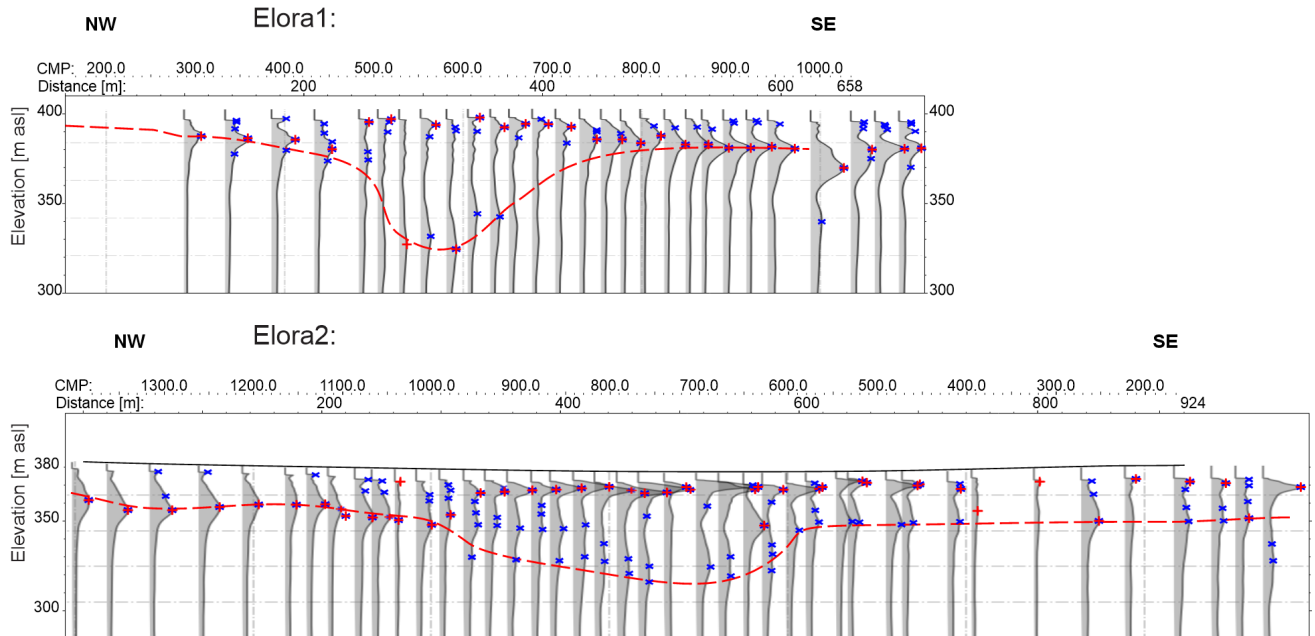


Figure 9. H/V amplitudes are displayed as shaded areas for the Elora1 and Elora2 profiles. The red dashed lines link the deepest H/V maxima and smoothly interpret the possible bedrock depth (VE ~1.5). Red crosses indicate maximum H/V amplitudes and blue x mark local maxima.

5.4 ARBORETUM HVSR DATA

The Arboretum HVSR profiles are different from the Elora profiles because the stiff near surface layer is absent at Arbo1 and almost too close to surface for its resolution in Arbo2. Many of the earliest signals have high H/V values (Figure 10).

Maximum HVSR amplitudes are variable at Arbo1, more pronounced peaks are found in the south where they occur at greater depth. The few observable local maxima are found in the south where sediments are thicker. Connecting H/V maxima leads to the interpretation of bedrock as an undulating surface between 5 and 30 m deep (Figure 10).

Along Arbo2, maximum values are found in the south at ~22 m depth. The signal character changes towards the north with flattening and deepening peaks in the center of the profile. The northern end is similar to the south with less pronounced peaks. Connecting maximum H/V leads to the interpretation of a 30 m deep buried valley covered by ~20 m of sediments. Very few local maxima are attributable to the deep valley floor of Arbo2 (Figure 10).

These are very encouraging results (Table 7), as it was anticipated that stiff, high-velocity near-surface layers would prevent deeper layers from creating a resonance. The different buried valley outlines are distinguishable by virtue of the deepest amplitude maxima.

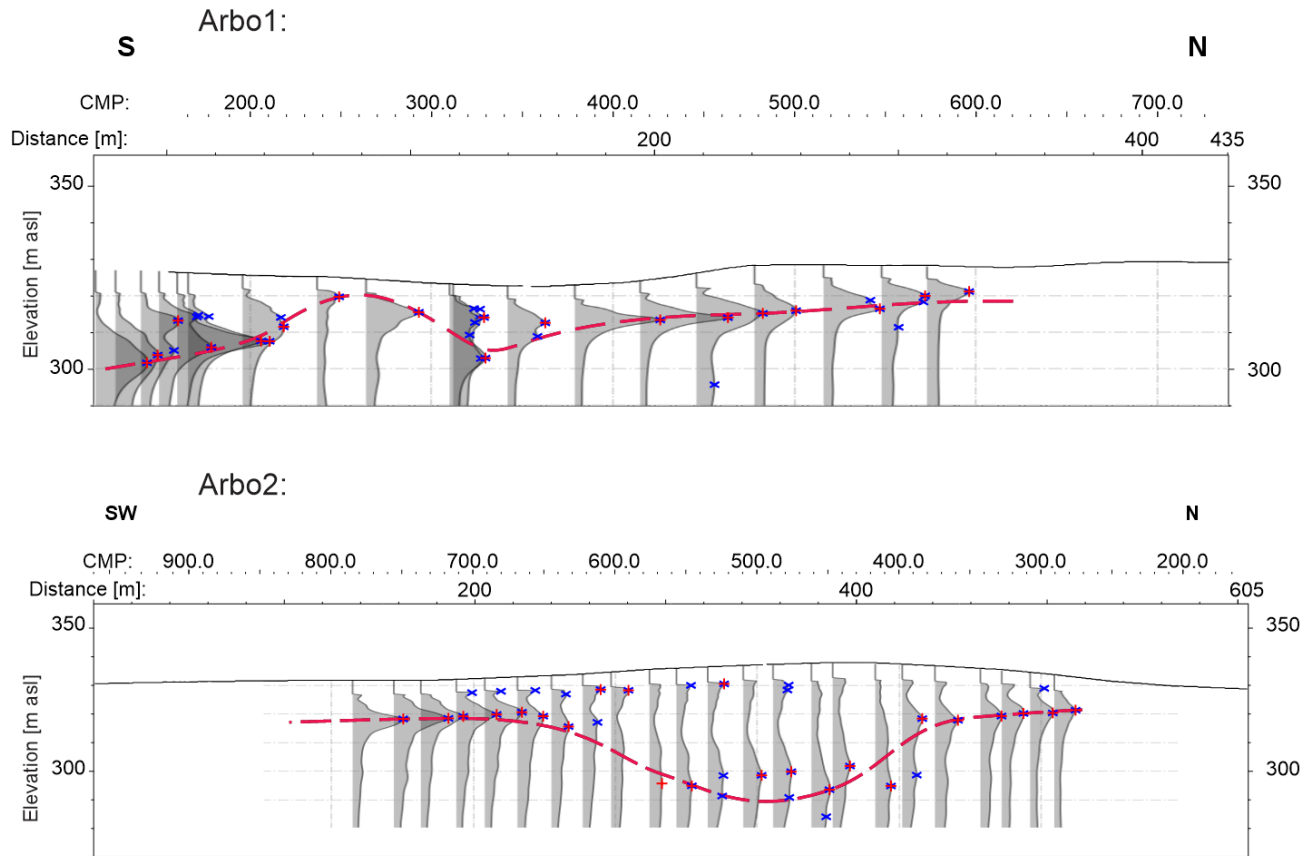


Figure 10. Shaded area H/V amplitude display for the Arbo 1 and 2 profiles. The red dashed lines connect the deepest H/V maxima and mark the interpreted bedrock depth (VE ~1.5). Red crosses indicate maximum H/V amplitudes and blue x mark local maxima.

Table 7: Comparison and highlights of HVSR profiles

Highlights	Elora1	Elora2	Arbo1	Arbo2
max amplitude	- very near surface - shallow bedrock - valley floor	- shallow till - shallow bedrock	- undulating bedrock - valley edge?	- shallow bedrock and till - valley floor
local maxima	- very near surface - valley floor	- shallow bedrock - valley floor	shallow bedrock	- very near surface - valley floor
valley width (m)	150	300	NA	250
valley floor depth (m)	75	55	NA	50
shallow bedrock depth (m)	15 - 20	20 to 30	5 to 15	10 to 15
valley fill, centre	not resolved	not resolved	NA	NA
valley fill, edges	not resolved	local max on northern edge	NA	NA

6. DISCUSSION

The seismic data interpretation presented in this report benefits from an examination of previously collected co-located geophysical datasets. A number of observations have arisen from these comparisons that set the stage for future research and are briefly discussed here; specifically, i) comparison of seismic reflection and HVSR data, ii) subjectivity of interpretation, and iii) differences between seismic and resistivity data.

6.1 COMPARISON AND INTEGRATION OF REFLECTION SEISMIC AND HVSR

Even though the two seismic methods are based on the same physical properties (material density and velocity), there are a number of differences in the character of the signal record. For both methods, the vertical resolution decreases with depth. The seismic reflection method has generally higher resolving power in the sub-metre to metre range whereas HVSR ranges from metres at the near surface to tens of metres at depth. No interpretable data was obtained from contacts between bedrock formations below the bedrock interface. Thin layers cannot be resolved with HVSR. The HVSR method might perform poorly where there are velocity reversals with depth. However, a low vertical resolution can be an advantage in a highly variable lithostratigraphic environment where seismic waves are scattered, and a reflection image is blurry. In this type of setting, HVSR can still provide a reliable H/V peak and a resonator depth, thereby aiding in seismic reflection interpretation (Dietiker et al. 2020b).

The bedrock signal can be compared for shallow depths outside of the valleys and deep areas within the valleys. Comparing H/V amplitudes (displayed as red shaded areas in Figure 11) with seismic reflections reveals good agreement between H/V maxima and bedrock reflections (red lines in Figure 11), specifically at both ends of the Elora1 profile. Generally, resonance peaks are within ± 5 m of reflection-interpreted depth to bedrock.

The valley outline (dashed black line connecting the deepest H/V maxima in Figure 11) is much smoother than interpreted from seismic reflections because the method estimates trends. There is subjectivity involved with the interpretation, and the exact outlines are influenced by the different scales of horizontal resolution: 1.5 m for seismic reflections and 15 to 20 m for HVSR. This leads to a narrower valley bottom interpretation for HVSR in Elora but the total valley width on both profiles is within ~ 20 m of the seismic reflection. The general depth of the valley matches bedrock reflections within 5 m.

There is a large mismatch between interpreted bedrock surfaces at the northern valley edge of Elora2 where reflections are characterised by reverberations (ringing) and HVSR shows moderate (~ 35 m) and deep (~ 50 m) local maxima inferring a much wider HVSR valley. HVSR maxima might point to the real valley bottom whereas the strongest seismic reflections stem from the valley fill. Further research

is needed to confirm this observation, but this might be another example of HVSR guiding seismic interpretation.

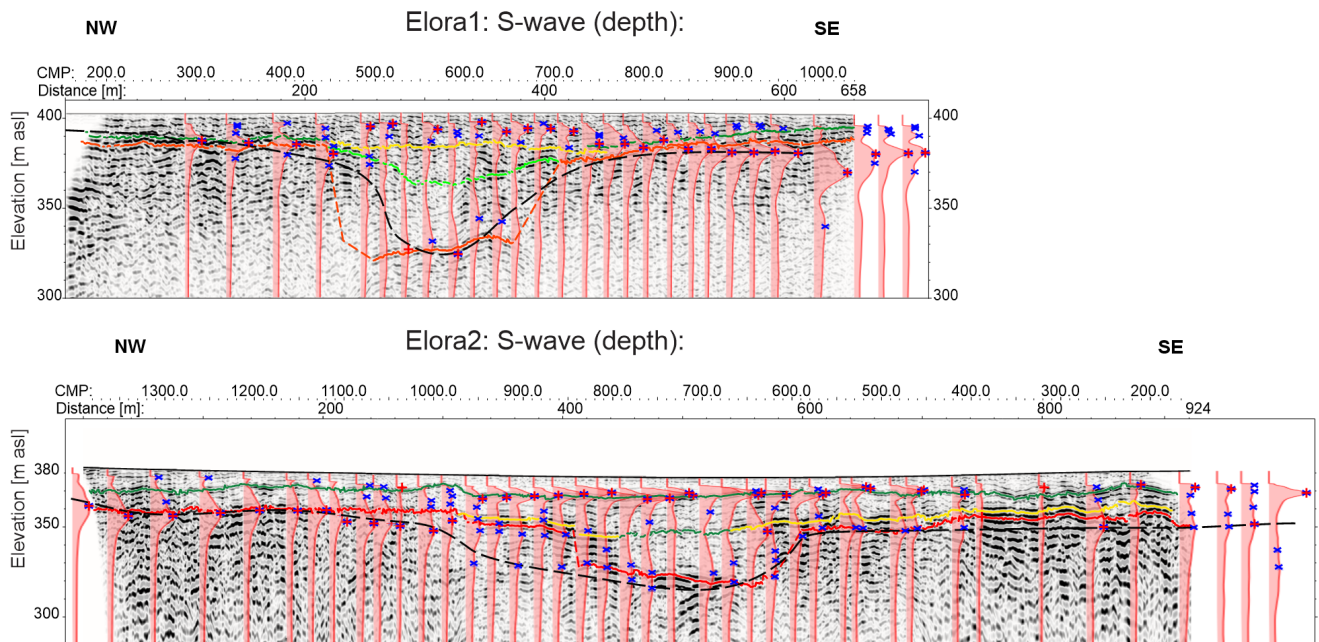


Figure 11. Seismic reflections are shown in grayscale with interpreted horizons marked by fine, coloured lines: red for bedrock, (light) green for tills and orange for shallow gravel, sand or till layers. H/V amplitudes are displayed as red shaded areas. The black dashed lines (red in Figure 9) smoothly link the deepest H/V maxima and interpret the possible bedrock depth ($VE=1.5$).

Despite the lower vertical resolution within the sediments, HVSR provides a signal response for a shallow horizon (~10 m) along the length of the Elora1 (a horizon not interpreted in the reflection section) and Elora2 profiles. This shallowest resonance in the centre of Elora2 can be attributed to the presence of the diamicton that was also detected by seismic reflections (likely Catfish Creek Till, green line in Figure 11 and 7). The depth difference between the methods is about two metres at this location. Considering the resolution limit and depth uncertainties associated with the HVSR method, the agreement between the two methods is encouraging.

The HVSR profile catches the south-facing slope of the bedrock depression (outlined by the dashed black line in Figure 12) at the southern end of Arbo1, whereas the seismic reflection data does not (limited by the roadway). Bedrock interpreted from seismic reflections and HVSR resonances match well along both profiles with vertical differences between HVSR and reflection horizons within 5 m, and lateral within 20 m (similar to those identified in the Elora profiles). Generally, HVSR results follow the trend of bedrock reflections within the buried valley delineated at Arbo2.

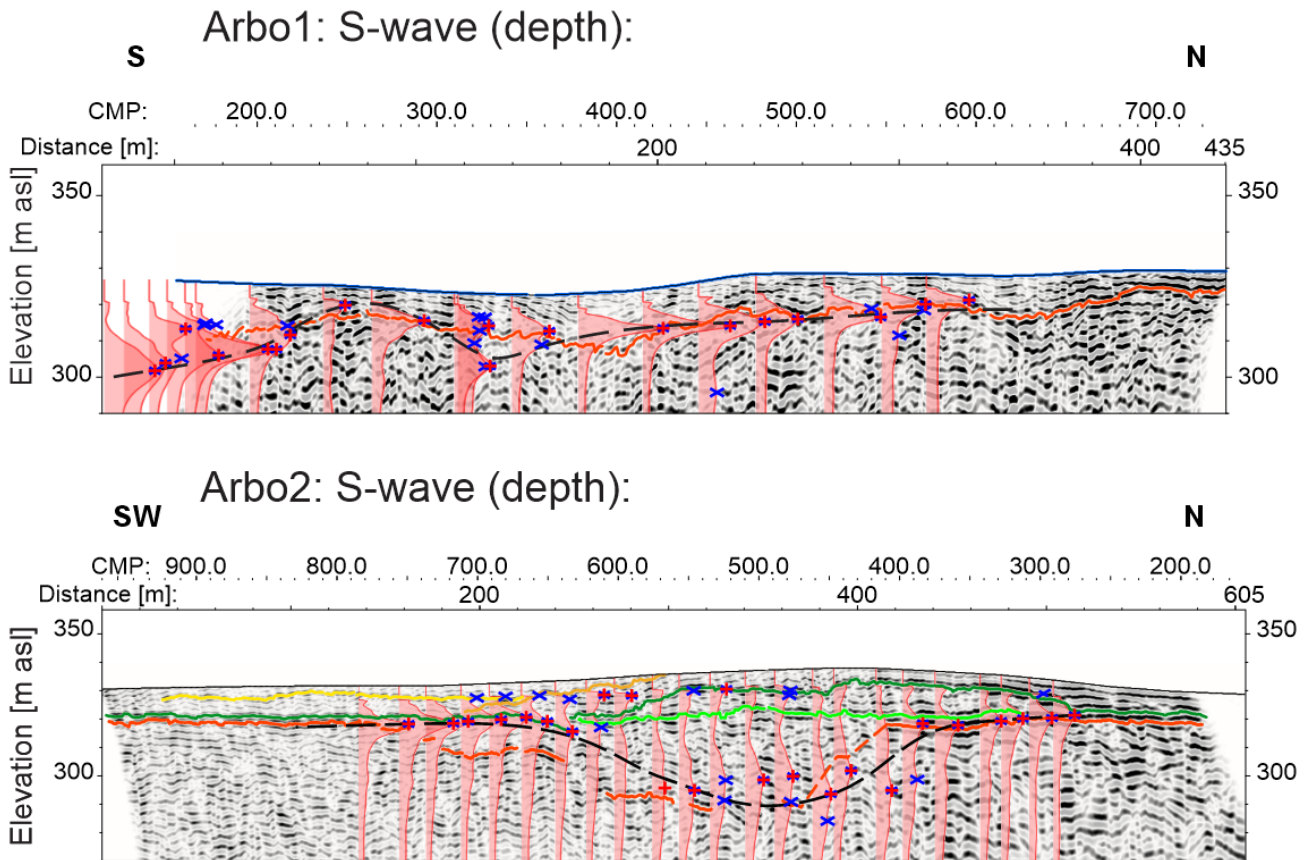


Figure 12. Seismic reflections for both Guelph profiles are shown in grayscale with interpreted horizons marked by fine, coloured lines (as per Figure 8 and 10). HVSR amplitudes are displayed as red shaded areas. The black dashed lines (red in Figure 10) smoothly link the deepest H/V maxima and mark bedrock depth (VE ~1.5).

In summary, both methods delineate the shallow bedrock surface and shallow firm layers in Guelph and Elora. Deep bedrock is also imaged with both methods, but the resolution is vastly different, with reflections providing much more detail. With adequately close station spacing, HVSR was shown here to provide reconnaissance information about the location of deeply buried valleys.

6.2 SUBJECTIVITY OF INTERPRETATIONS

Although seismic reflection interpretation is based on measurable quantities such as reflection strength and continuity, experience and geological knowledge influence the process immensely resulting in multiple possible interpretations.

One of the main goals of this survey was the delineation of the buried valley shape. Because of the very steep angle of the valley edges, however, reflections could not define the bedrock wall geometry. The slopes were interpolated between the defined deep valley floor and shallow bedrock, supported by information from discontinuities within the valley fill. Three possible scenarios are presented, each of which can be justified by one of the datasets (Figure 13).

The interpretation presented earlier in Figures 6 and 7 is represented in Figure 13B. Different interpretations are possible regarding i) the valley width, ii) steepness of the valley margin, and iii) the depth of shallow bedrock beyond the buried valley (indicated in Figure 13C, D).

A key observation is that there are strong reflections extending into the valley from the edges. This could be interpreted as the presence of diamicton on either side of the valley, as the strong impedance contrast at the top of the diamicton reduces the reflection amplitudes from bedrock below. The NW valley edge could dip less steeply, but even at $\sim 45^\circ$ it creates uninterpretable reflections. An important observation is that the sediments in the valley centre have chaotic, low-amplitude reflections, but differ significantly from the character of the reflections at the valley edges. Figure 13C additionally shows amplitude information from HVSR, and a valley outline obtained from HVSR maxima (dark blue, introduced in Figure 8). Based on partial absence of reflection continuity of the valley fill, a secondary erosion event could be postulated (marked by light blue subvertical edges, CMP 500 and 600).

Even though the HVSR method has lower resolution than seismic reflection, there are a couple of interpretive points to be noted from the addition of HVSR information: (i) a steeper northern valley wall is a more likely scenario based on HVSR maxima, and (iii) the shallower bedrock surfaces interpreted from the reflection data are a better match to the HVSR amplitude maxima. This demonstrates the value of HVSR to aid in seismic reflection interpretation. It also suggests the value of HVSR for reconnaissance purposes.

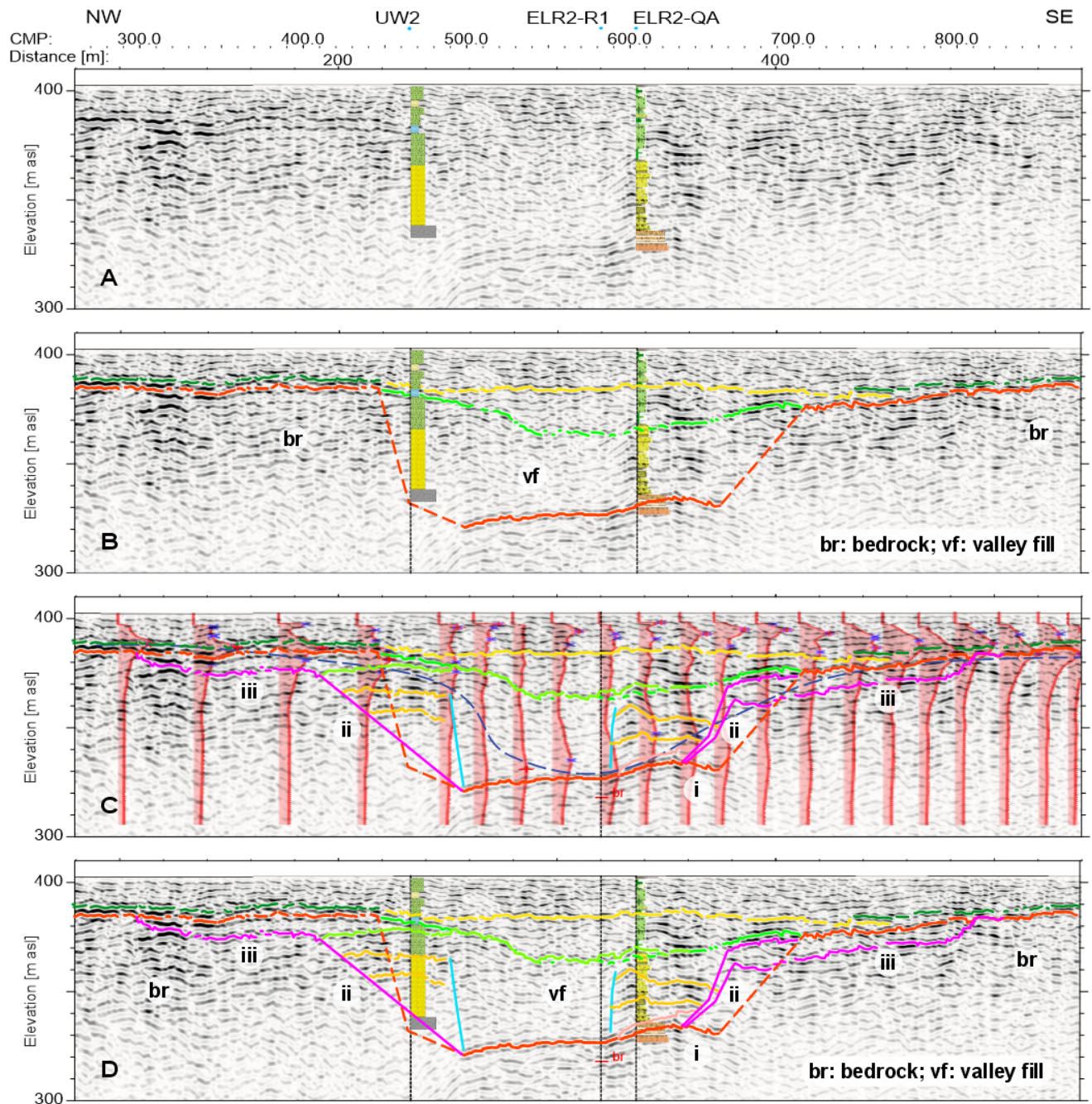


Figure 13. Three interpretations of bedrock depth and valley margins at Elora1 – Road6N. A) uninterpreted seismic reflection, B) interpreted seismic reflection as in Figure 6 and 7, C) HVSr signal overlay and three alternative interpretations (pink): i) narrower valley floor, ii) different valley wall inclination, and iii) deeper bedrock surface, D) multiple interpretations as described in C. VE = 1.

6.3 DIFFERENCES BETWEEN REFLECTION IMAGES AND RESISTIVITY MODELS

Resistivity and seismic reflection methods differ in both lateral and vertical resolution capabilities. They also measure different physical properties. Resistivity is indirectly sensitive to the combined effect of sediment materials, porosity and pore-fluid conductivity, while the reflections stem from contrasts in

material density and velocity. A change in density does not necessarily coincide with a material change, for example variable compaction creates an acoustic-impedance change and thereby a reflection. Alternatively, materials with different resistivities could have similar densities. The process of model building also differs substantially. The seismic-reflection method depends on direct measurements and display of travel times, while resistivity models are based on the more indirect process of model fitting or inversion of measurements, a process affected by non-uniqueness, choice of parameters and starting model.

The seismic profiles are in general accord with the ground and airborne resistivity inversion models (Conway-White et al., 2023; Steelman et al., 2018). The potential methods' inherent tendency to smooth features results in a resistivity model with smoother valley definitions than what is interpreted from the seismic reflections.

For both Elora transects, airborne and ground resistivity models show good agreement with interpreted seismic reflections for the shallower bedrock interface. The buried valley shape of Elora1 is very similar in depth and lateral extent to the interpreted seismic image. For Elora2 the interpreted valley shape and depth to bedrock is different. The Elora2 reflection image shows greater similarity with the airborne resistivity model (steep sidewalls) than to the surface resistivity model that has a less well-defined valley and greater bedrock depth variability (Conway-White et al. 2022; Conway-White et al., 2023).

Both resistivity and seismic methods highlight the variable character of the Elora valley fill in the centre compared to the edges. Both resistivity models show lower resistivity values in the centre of the valley, together with the low-amplitude, chaotic seismic reflections coinciding with higher resistivity as distinct from the continuous high-amplitude reflections near the edges.

These studies indicate the value of the Guelph and Elora buried-valley sites as ideal ongoing field laboratories for comparison of the strengths and weaknesses of different geophysical methods together with continuously cored high-quality borehole information.

7. CONCLUSION

Geophysical methods play an important role in groundwater research as they provide subsurface information non-intrusively at an excellent cost-to-information ratio. This report presents results of two seismic methods operating at different levels of detail and cost. Microtremor HVSR is an easily deployed, rapid, inexpensive reconnaissance tool for estimating depth to bedrock and thus delineating buried valley locations, even in challenging and complex geological terrain containing a number of dense diamicton units. HVSR may also aid in seismic-reflection data interpretation. The seismic-reflection profiles have provided detailed, high-resolution images of the buried valleys that are 200 m wide and 30 to 60 m deep in the Elora-Fergus and Guelph areas.

8. ACKNOWLEDGMENTS

With appreciation for the collaboration and field coordination of Drs. Peeter Pehme, Colby Steelman, and Beth Parker. We thank Oliver Conway-White, Connor Gorrie, and Nataly Aranda for their support during field acquisition. Thanks to Dr. Greg Oldenborger (GSC) for his review of this report. The research was a collaboration between the Geological Survey of Canada, the Morwick G360 Groundwater Research Institute [Memorandum of Understanding (MOU) AGR-5252-IA1 2021], and the University of Waterloo. This study was supported by the Geological Survey of Canada (Natural Resources Canada) under the Groundwater Geoscience program's Archetypical Aquifer project 2019-2024.

9. REFERENCES

- Ahern T., Casey R., Barnes D., R., Knight T., and Trabant C. 2012. Seed Reference Manual, Incorporated Research Institutions for Seismology (IRIS), Washington, D.C., 220 pp., available at <https://www.fdsn.org/publications> (last accessed March 2021).
- Bonnefoy-Claudet, S., Kohler, S., Cornou, C., Wathelet, M., and Bard, P. Y. 2008. Effects of Love waves on micro-tremor H/V ratio: *Bulletin of the Seismological Society of America*, 98, 288–300, doi: 10.1785/0120070063.
- Bajc, A.F., Russell, H.A.J., Sharpe, D.R., 2014. A three-dimensional hydrostratigraphic model of the Waterloo Moraine area, southern Ontario, Canada. *Canadian Water Resources Journal* 39, 95–119. <https://doi.org/10.1080/07011784.2014.914794>
- Barnett, P.J. 1992. Quaternary geology of Ontario; in *Geology of Ontario*. Ontario Geological Survey, Special Volume 4, Part 2, p. 1011-1090.
- Brewer, K., Cartwright, T., Pugin, A.J.-M. 2013. The microvibe a new multicomponent portable seismic vibrator. *Symposium on the Application of Geophysics to Engineering and Environmental Problems; Proceedings: 266-269*. <https://doi.org/10.4133/sageep2013-028.1>.
- Brunton, F.R. and Brintnell, C. 2020. Early Silurian sequence stratigraphy and geological controls on karstic bedrock groundwater-flow zones, Niagara Escarpment region and the subsurface of southwestern Ontario; Ontario Geological Survey, Groundwater Resources Study 13.
- Burt, A.K. 2015. Quaternary stratigraphy of the Niagara Peninsula revealed with three-dimensional mapping. In *Summary of Field work and other Activities, 2015*. Ontario Geological Survey, Open File Report, 6313: 35-1 to 35-17.
- Burt, A.K. and Dodge, J.E.P. 2016. Three dimensional modelling of surficial deposits in the Orangeville-Fergus area of Southern Ontario. Ontario Geological Survey, Groundwater Resources Study 15, 155 pp.
- Castellaro, S. and Mulargia, F. 2009. The Effect of Velocity Inversions on H/V. *Pure applied geophysics*, 166: 567–592. <https://doi.org/10.1007/s00024-009-0474-5>
- Castellaro, S., Mulargia, F., and Bianconi, L. 2005. Passive Seismic Stratigraphy: A new efficient, fast and economic technique. *Stratigrafia sismica passiva: una nuova tecnica accurata, veloce ed economica*. *J. Geotech. Environ. Geol.* 3: 51–77.
- Chandler, V.W. and Lively, R. S. 2016. Utility of the horizontal-to-vertical spectral ratio passive seismic method for estimating thickness of Quaternary sediments in Minnesota and adjacent parts of Wisconsin. *Interpretation* 4 (3): SH71–SH90. <https://doi.org/10.1190/INT-2015-0212.1>
- Cole, J., Coniglio, M., and Gautrey, S., 2009. The role of buried bedrock valleys on the development of karstic aquifers in flat-lying carbonate bedrock: insights from Guelph, Ontario, Canada. *Hydrogeol J* 17, 1411–1425. <https://doi.org/10.1007/s10040-009-0441-3>
- Conway-White, O. 2020. Lithostratigraphic characterization of a buried bedrock valley using airborne and surface geophysics. MSc Thesis, The University of Guelph
- Conway-White, O., Steelman, C.M., Smiarowski, A., Ugalde, H., Endres, A.L., Arnaud, E., and Parker, B.L. 2022. Improving spatial characterization of buried bedrock valleys through airborne frequency-domain electromagnetic, residual magnetic and surface resistivity measurements. *Journal of Applied Geophysics*, 199: 104584. doi:10.1016/j.jappgeo.2022.104584.104584.

- Conway-White, O., Steelman, C.M., Arnaud, E., Ugalde, H., Munn, J.D., Parker, B.L., 2023. Constraining the lithostratigraphic architecture of a buried bedrock valley using surface electrical resistivity and seismic refraction tomography. *Can. J. Earth Sci.* 60: 333–349 (2023) | [dx.doi.org/10.1139/cjes-2021-0062](https://doi.org/10.1139/cjes-2021-0062)
- Crow, H. L., Hunter, J. A., and Motazedian, D. 2011. Monofrequency *in situ* damping measurements in Ottawa area soft soils; *Journal of Soil Dynamics and Earthquake Engineering*, v.31, p. 1669-1677. <https://doi.org/10.1016/j.soildyn.2011.07.002>
- Crow, H. L., Hunter J. A., Olson, L.C., Pugin A.J.-M., and Russell H.A.J. 2018. Borehole geophysical log signatures and stratigraphic assessment in a glacial basin, southern Ontario. *Canadian Journal of Earth Sciences*. 55(7): 829-845. <https://doi.org/10.1139/cjes-2017-0016>
- Dietiker, B., Hunter, J. A., Pugin, A. J.-M., Crow, H.L., Mallozzi, S., Brewer, K., and Cartwright, T. 2018. HVSR measurements in complex sedimentary environment and highly structured resonator topography – comparisons with seismic reflection profiles and geophysical borehole logs. *Symposium on the Application of Geophysics to Engineering and Environmental Problems; Proceedings*: 324-330. <https://doi.org/10.4133/sageep.31-025>
- Dietiker, B. and Hunter, J.A. 2019. HVSR measurements of two-dimensional subsurface structures – comparisons with seismic reflection profiles. *Symposium on the Application of Geophysics to Engineering and Environmental Problems; Proceedings*: 266-269. <https://doi.org/10.4133/sageep.32-056>
- Dietiker, B., Hunter, J. A., and Pugin, A.J.-M. 2020a. Improved analysis of Horizontal-to-Vertical Spectral Ratio measurements for groundwater investigations. In Russell, H.A.J. and Kjarsgaard, B.A. Eds. *Southern Ontario groundwater project 2014–2019 summary report*. Geological Survey of Canada, Open File 8536. <https://doi.org/10.4095/321101>
- Dietiker, B., Pugin, A.J.-M., Hunter, J.A. 2020b. Combined Shear-Wave Seismic Reflection and H/V Spectral Ratio Surveys - A Case Study. Abstract in NSG2020 26th European Meeting of Environmental and Engineering Geophysics, Dec 2020, Volume 2020, p.1 - 5. <https://doi.org/10.3997/2214-4609.202020067>
- Dobry, R., Oweis, I., and Urzua, A. 1976. Simplified procedures for estimating the fundamental period of a soil profile. *Bulletin of the Seismological Society of America*, v. 66, No.4.
- Etris, E.L., Crabtree, N. J., and Dewar, J. 2002. True Depth Conversion: More Than a Pretty Picture. *csegrecorder*, NOV 2002, vol. 26 no. 09
- Evans S. G. and Brooks, G.R. 1994. An earthflow in sensitive Champlain Sea sediments at Lemieux, Ontario, June 20, 1993, and its impact on the South Nation River. *Canadian Geotechnical Journal*, 1994, 31(3): 384-394. <https://doi.org/10.1139/t94-046>
- Fäh, D., Kind, F., and Giardini, D. 2001. A theoretical investigation of average H/V ratios: *Geophysical Journal International*, 145, 535–549. <https://doi.org/10.1046/j.0956-540x.2001.01406.x>
- Hilton, S.W 1978. The Elora-Fergus buried valley: further geophysical studies, MSc Thesis, Department of Earth Sciences, The University of Waterloo.
- Gao, C., 2011. Buried bedrock valleys and glacial and subglacial meltwater erosion in southern Ontario, Canada. *Canadian Journal of Earth Sciences* 48, 801–818. <https://doi.org/10.1139/e10-104>
- Greenhouse, J.P. and Karrow P. F. 1994. Geological and geophysical studies of buried valleys and their fills near Elora and Rockwood, Ontario. *Canadian Journal of Earth Sciences*. 31(12): 1838-1848. <https://doi.org/10.1139/e94-163>

- Hunter, J.A. and Crow, H. L. eds. 2012. Shear Wave Velocity Measurement Guidelines for Canadian Seismic Site Characterization in Soil and Rock. Geological Survey of Canada, Open File 7078, 227 p.
- Hunter, J. A., Crow, H. L. Brooks, G. R. Pyne, M.Motazedian, D. Lamontagne, M. Pugin, A. J.-M., Pullan, S. E. Cartwright, T. Douma, M. Burns, R. A. Good, R. L. Kaheshi-Banab, K. Caron, R. Kolaj, M. Folahan, I. Dixon, L. Dion, K. Duxbury, A., Landriault, A., Ter-Emmanuil, V., Jones, A., Plastow, G., and Muir, D. 2010a. Seismic site classification and site period mapping in the Ottawa area using geophysical methods. Geological Survey of Canada, Open File 6273, 80 pages. <https://doi.org/10.4095/286323>
- Hunter J. A., Burns, R. A., Good, R. L., Pullan, S. E., Pugin, A. J.-M., and Crow, H. L. 2010b. Near-surface geophysical techniques for geohazards investigations: some Canadian examples. *Lead Edge* 29(8):936–947. <https://doi.org/10.1190/1.3480011>
- Ibs-von Seht, M., and Wohlenberg, J. 1999. Microtremor measurements used to map thickness of soft sediments. *Bull. Seismol. Soc. America*, 89: 250-259. <https://doi.org/10.1785/BSSA0890010250>
- Karrow PF (1968) Pleistocene geology of the Guelph area. Geological Report 61, accompanied by map 2153, scale 1:63,360, Ontario Department of Mines, Toronto.
- Karrow, P. 1987. Quaternary Geology of the Hamilton-Cambridge Area. Ontario Geological Survey Report 255, Ministry of Northern Development and Mines.
- Karrow, P.F., 1974. Till Stratigraphy in parts of southwestern Ontario. *Geological Society of America Bulletin* 85, 761–768. [https://doi.org/10.1130/0016-7606\(1974\)85<761:TSIPOS>2.0.CO;2](https://doi.org/10.1130/0016-7606(1974)85<761:TSIPOS>2.0.CO;2)
- Konno, K. and Ohmachi, T. 1998. Ground-motion characteristics estimated from spectral ratio between horizontal and vertical components of microtremor. *Bulletin of the Seismological Society of America*, 88: 228–241. <https://doi.org/10.1785/BSSA0880010228>
- Lachet, C. and Bard, P. Y. 1994, Numerical and theoretical investigations on the possibilities and limitations of Nakamura's technique: *Journal of Physics of the Earth*, 42, 377–397, doi: 10.4294/jpe1952.42.377.
- Maldaner, C.H., Munn, J.D., Coleman, T.I., Molson, J.W., Parker, B.L., 2019. Groundwater flow quantification in fractured rock boreholes using active distributed temperature sensing under natural gradient conditions. *Water Resources Res.* 55 (4), 3285-3306.
- Matsushima, S., Hirokawa, T., De Martin, F., Kawase, H., and Sánchez-Sesma, F. 2014. The Effect of Lateral Heterogeneity on Horizontal-to-Vertical Spectral Ratio of Microtremors Inferred from Observation and Synthetics. *Bulletin of the Seismological Society of America*; 104: 1, 381–393. <https://doi.org/10.1785/0120120321>
- Molnar S., Cassidy, J. F., Castellaro, S., Cornou, C., Crow, H. L., Hunter, J. A., Matsushima, S., Sánchez-Sesma, F., and Yong, A. 2018. Application of Microtremor Horizontal-to-Vertical Spectral Ratio (MHVSR) Analysis for Site Characterization: State of the Art. *Surveys in Geophysics*. doi.org/10.1007/s10712-018-9464-4
- Motazedian D., Hunter, J.A., Pugin, A. J.-M., and Crow, H. L. 2011. Development of a Vs30 (NEHRP) map for the city of Ottawa, Ontario, Canada. *Can Geotech J* 48:458–472. <https://doi.org/10.1139/T10-08>
- Munn, J.D., Maldaner, C.H., Coleman, T.I., Parker, B.L. (2020) Measuring fracture flow changes in a bedrock aquifer due to open hole and pumped conditions using active distributed temperature sensing, *Water Resources Research*, 56, e2020WR027229. <https://doi.org/10.1029/2020WR027229>

- Nakamura, Y. 1989. A method for dynamic characteristics estimation of subsurface using microtremor on the ground surface: Quarterly Report Railway Technical Research Institute, 25–30. <http://www.rtri.or.jp/eng/>
- Nakamura, Y. 2000. Clear identification of fundamental idea of Nakamura's technique and its applications: Presented at the 12th World Conference on Earthquake Engineering.
- Nogoshi, M. and Igarashi, T. 1971. On the amplitude characteristics of microtremor (part 2) (in Japanese with English abstract): Journal of the Seismological Society of Japan, 24, 26–40.
- Ontario, Ministry of Mines. 2012. Surficial geology of Southern Ontario. Accessed July 2023 at <https://data.ontario.ca/dataset/surficial-geology-of-southern-ontario>
- Pugin, A.J.-M., K. Brewer, T. Cartwright, S. E. Pullan, D. Perret, H. L. Crow, and Hunter, J. A. 2013. Near surface S-wave seismic reflection profiling—new approaches and insights. First Break EAGE 31:49–60. <https://doi.org/10.3997/1365-2397.2013005>
- Pullan, S.E., Hunter, J.A., Russell, H.A.J., Sharpe, D.R. 2004. Delineating buried-valley aquifers using shallow seismic reflection profiling and downhole geophysical logs - An example from southern Ontario, Canada, in: Progress in Environmental and Engineering Geophysics: Proceedings of the International Conference on Environmental and Engineering Geophysics, ICEEG 2004. pp. 39–43.
- Russell, H.A.J., Hinton, M.J., van der Kamp, G., Sharpe, D.R., 2004. An overview of the architecture, sedimentology and hydrogeology of buried-valley aquifers in Canada. Proceedings of the 57th Canadian Geotechnical Conference and the 5th joint CGS-IAH Conference 2B (26-33). <https://doi.org/10.4095/215602>
- Russell, H.A.J., Sharpe, D.R., Cummings, D.I., 2007. A framework for buried-valley aquifers in southern Ontario, in: Proceedings of the 60th Annual Canadian Geotechnical Society (CGS) and 8th Joint Canadian National Chapter of the International Association of Hydrogeologists (IAH-CNC) Groundwater Specialty Conference. Canadian Geotechnical Society and International Association Hydrogeologists, pp. 386–393.
- SESAME 2004. Guidelines for the implementation of the H/V spectral ratio technique on ambient vibrations-measurements, processing and interpretation. SESAME European research project, Deliverable D23. 12., Project No. EVG1-CT-2000-00026 SESAME, 62 pp.
- Society of Exploration Geophysicists. 2017. "Announcements" The Leading Edge 36: 449–449. <https://doi.org/10.1190/tle36050449.1>
- Stelman, C. M., Arnaud, E., Pehme, P., and Parker, B. L. 2018. Geophysical, geological, and hydrogeological characterization of a tributary buried bedrock valley in southern Ontario. Canadian Journal of Earth Sciences, 55(7), 641-658. <https://doi.org/10.1139/cjes-2016-0120>
- Spencer, J.W. 1881. Discovery of the pre-glacial outlet of the basin of Lake Erie into that of Lake Ontario; with notes on the origin of our lower Great Lakes. Proceedings of the American Philosophical Society, 19: 300–337.

Appendix 1: DATA PROCESSING

A1.1 SEISMIC REFLECTION DATA

A1.1.1 PROCESSING

The raw shot records from the acquisition were processed in the first step to yield optimal high-resolution reflections in time domain (two-way travel-time). The processing steps were applied as listed in Table A1. The resulting P- and S-wave profiles are provided in large format in Appendix A2.

After processing, the following observations were made on the topo-corrected time sections:

- The shallowest reflection in the P-wave section is created by the water table (Figure A1) where the P-wave velocity (V_p) abruptly increases to 1450 m/s which is the velocity of water.
- The complex stratigraphy with a high-velocity till at surface produces strong surface waves. It was necessary to suppress these strong signals with the application of bandpass and frequency-wavenumber-filtering (fk) to enhance the underlying reflections (Table A2, Figure A2).

Table A1. Processing steps applied to the four Guelph and Elora seismic reflection profiles.

Initial processing (all data)	
Format conversion, SEG2 to KGS SEGY	
Pilot trace based cross-correlation	
Separation of V, H1, H2 components	
Frequency filter	
Applying of geometry	
Statics calculation (refraction analysis)	
Common midpoint (CMP) sorting	
P-Wave V component (250 ms)	S-Wave H2 component (1000 ms)
Refraction static correction	fk- and bandpass filter
fk- and bandpass filter	Scaling (trace normalization)
Scaling (trace normalization)	Top mute (P-, surface waves)
Bottom mute (S-, surface waves)	
Velocity semblance analysis	Velocity semblance analysis
NMO corrections	NMO corrections
Stacking	Stacking
Topography correction	Topography correction
Time to depth conversion	Time to depth conversion

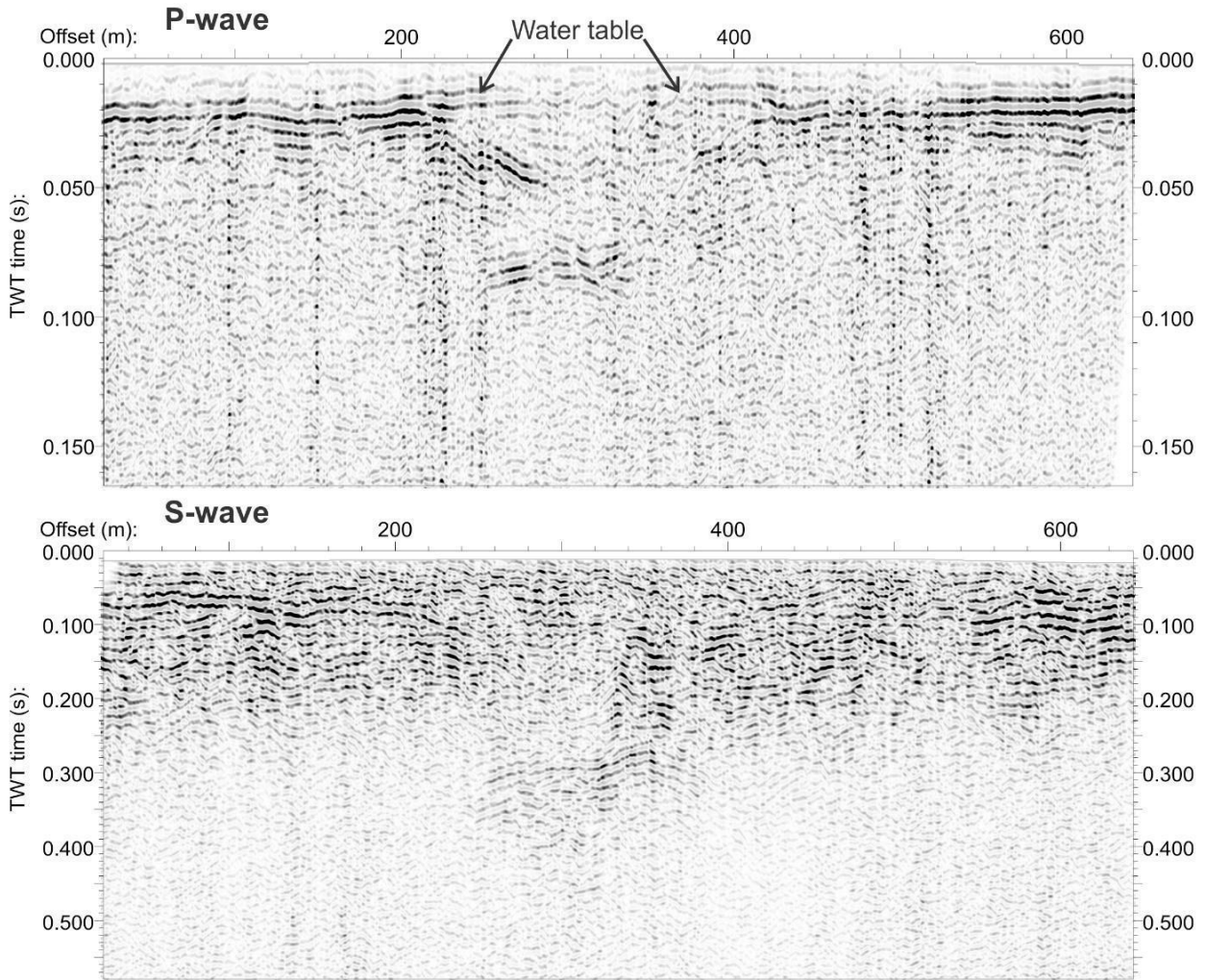


Figure A1. Time-domain sections of Elora1 – Road6N illustrating the difference between P-wave reflections (top) and S-wave sections (bottom), most notably the water table reflection seen only on the P-wave profile.

Table A2: Summary of applied filter parameters.

Profile	Filter type	Start	End		
P-wave (all)	bandpass (bp)	100 Hz	400 Hz		
S-wave (all)	bandpass (bp)	40 Hz	160 Hz		
		Velocity range (m/s)	Time scale	Space scale	Tapering (%)
Elora1	fk	192 - 637	1	2	28
Elora2	na				
Arbo1	fk	171 - 348	1	2	28
Arbo2	fk	164 - 803	1	2	28

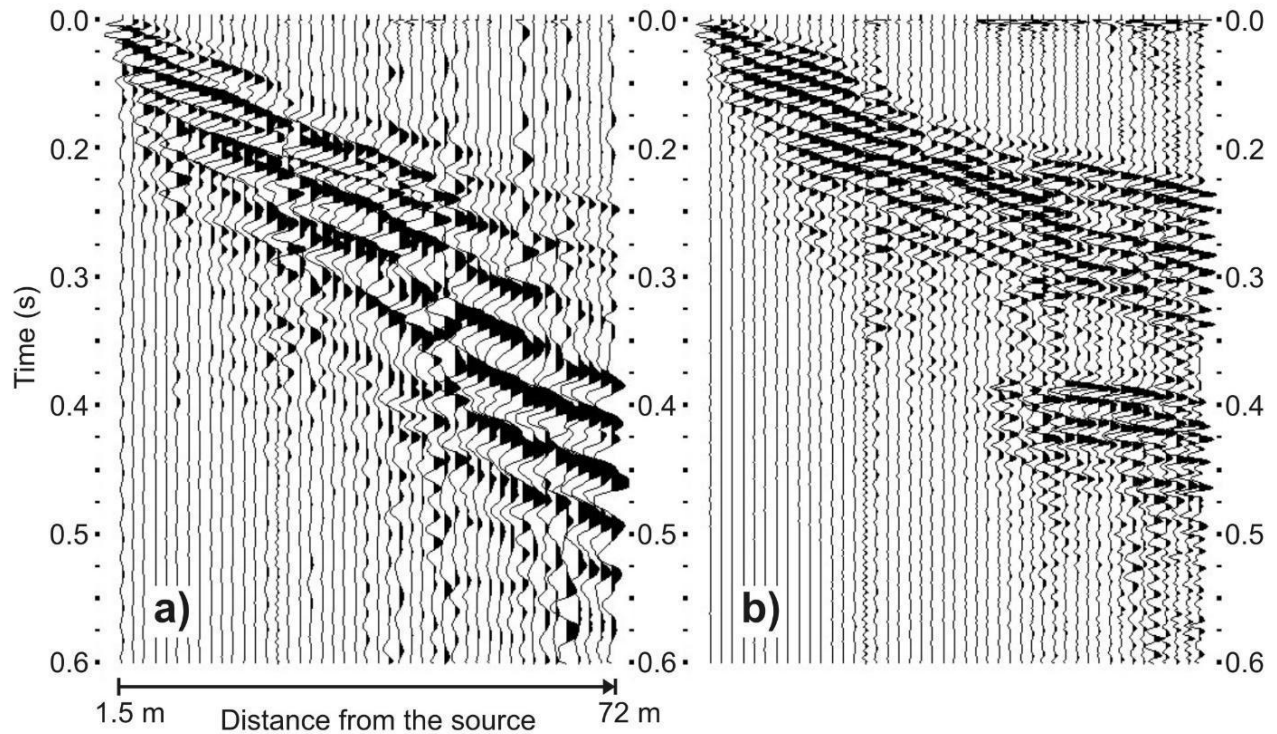


Figure A2. Shot record acquired along Elora1 – Road6N over the buried valley: a) Raw correlated record with dominant surface waves. b) After application of bandpass and fk filtering (see Table A2 for filter parameters) enhancing dominant reflections. High surface-wave amplitudes result from the shallow, high-velocity till in the area.

A1.1.2 DEPTH CONVERSION

As part of the reflection processing, a velocity-semblance analysis was carried out to provide stacking velocities needed to correct the normal-moveout (NMO) of the reflections. This is necessary because the traveled distance of reflected waves increases hyperbolically with offset (x): $T = \sqrt{T_0 + x^2/v^2}$ (Figure A3).

The stacking velocities, also referred to as “average” velocities were used to calculate single-layer or interval velocities (V_{int}) which provide information about the subsurface at analyzed CMP gathers and reflection arrival times (layer boundaries). Figure A4 displays interval shear-wave velocities for Elora1-Road6N on the left, linearly interpolated interval velocities in the centre and the velocity model used for depth conversion on the right.

The interval velocities (also shown in all Figures of Appendix 2) were used to create a velocity model for the time-to-depth conversion of the reflection data. Generally, the best ties to borehole information are achieved when NMO velocities are reduced to ~80 % of their original values for model creation. Etris et. al. (2002) explain in detail why original NMO velocities cannot be used for the best depth conversion.

The simplified velocity model (Figure A4, right) was adjusted such that the best matches for selected horizons and borehole information were reached. Figure A5 shows the reflection profiles of Elora1 – Road6N as time section on the left and after depth conversion on the right. Note how the velocities were increased to match bedrock reflections to recorded bedrock depth of well ELR2-R2 and decreased to

match ERL2-R1. Not only the bedrock horizon-to-well tie needs to be correct, but also different horizons between P- and S-wave sections. As depth conversion relies on interpreted horizons, depth conversion and interpretation are performed simultaneously to accommodate the influence each have on the other.

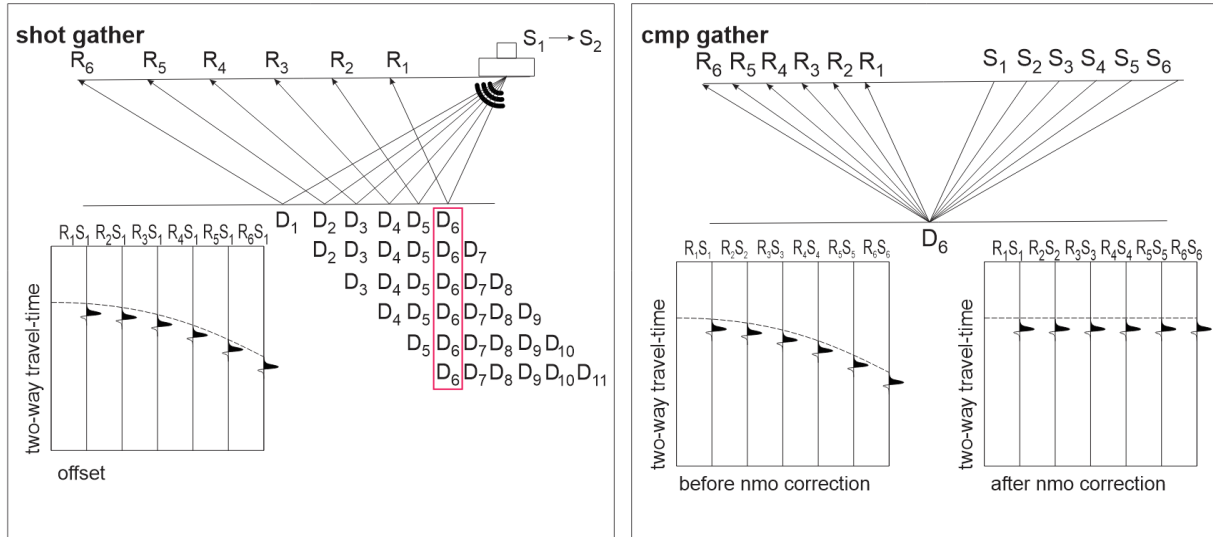


Figure A3. Geometrical explanation of normal-moveout in a common mid-point (CMP) gather.

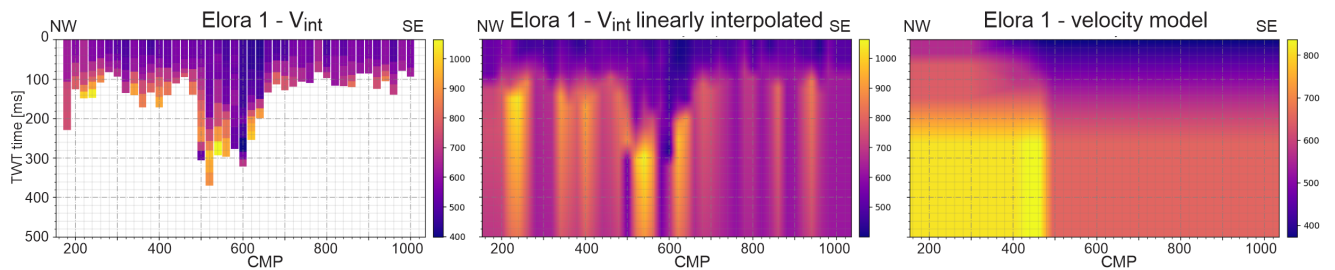


Figure A4. Elora 1 - Road6N velocities: Left – V_{int} : Interval velocities from semblance analysis of every 20th CMP gather; Center – linearly interpolated interval velocities; Right - velocity model simplified from V_{int} as used for the depth conversion.

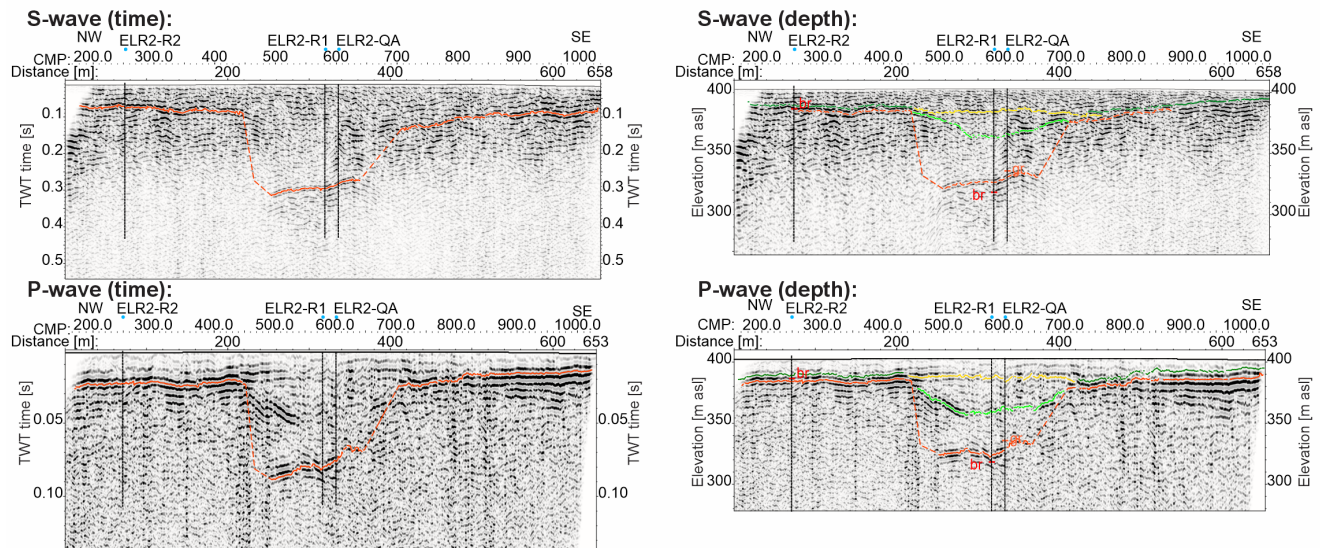


Figure A5. Eloral – Road6N time (left) and depth (right) sections. S-wave depth section was created using the velocity model from Figure A4.

A1.2 HVSr DATA

A1.2.1 HVSr METHOD EXPLAINED

The Microtremor Horizontal-to-Vertical Spectral Ratio (HVSr) method detects minuscule ground movements (on the order of micrometres per second) with the aim of identifying amplifications of these motions at particular frequencies (Konno and Ohmachi, 1998). It is debated which motions (surface waves, Rayleigh, Love, Airy waves) contribute to microtremors as documented by Lachet and Bard (1994); Nakamura, (2000); Fäh et al. (2001); Bonnefoy-Claudet et al. (2006). The frequency spectra of these ground motions vary depending on sediment type and structure of the subsurface at the immediate measurement site, leading to amplification (resonance) at a fundamental frequency (Konno and Ohmachi, 1998). For geotechnical assessments the resonance frequency is used to infer shear-wave velocity and depth to firm ground (e.g., bedrock; Hunter and Crow, 2012).

HVSr can provide information about the continuity of subsurface horizons when measurement points are closely spaced, and information can be extrapolated from point to point. Figure A6 shows three sample points from Line 6N with distinctly different signatures along the line from NW to SE. The strongest resonance peak (H/V amplitude = 4.2) occurs at a frequency of 12.2 Hz (Figure A6a). Further along the profile (187m), resonance drops to 2.9 Hz with a lower H/V amplitude of 2.7 (Figure A6b); secondary peaks (local maxima) between 5 and 18 Hz with relatively moderate H/V amplitudes are visible, which may stem from layered near-surface sediments at this location, as higher frequencies mean shallower depths. A return to strong near-surface resonance of 19.7 Hz (H/V amplitude = 4) at station 12 (Figure A6c) is linked to a competent layer, interpreted to be till. A lower amplitude peak (local maxima) at 2.9 Hz originating from a greater depth may stem from deep bedrock. This small resonance at 2.9 Hz (and another at 4.4 Hz) correlates closely with peaks of the H/V curve at site L6N-08, but without the information from other sites along the profile, the deep resonance interpreted at L6N-12 would likely be given less significance.

The highest amplitude (peak) occurs at the fundamental or resonance frequency (f_0) which is related to the average shear-wave velocity and the overlying sediment thickness, from which bedrock depth is inferred. The resonance is created in the sediment layer by a strong contrast in density and shear-wave velocity between two layers (e.g., sand over bedrock). Estimation of depth to bedrock can be confounded

by shallower units that also have a high-amplitude response like layers of diamicton. Such layers can mute responses from deeper underlying horizons, particularly if the intervening distance is small (e.g., a thin layer of till overlying bedrock).

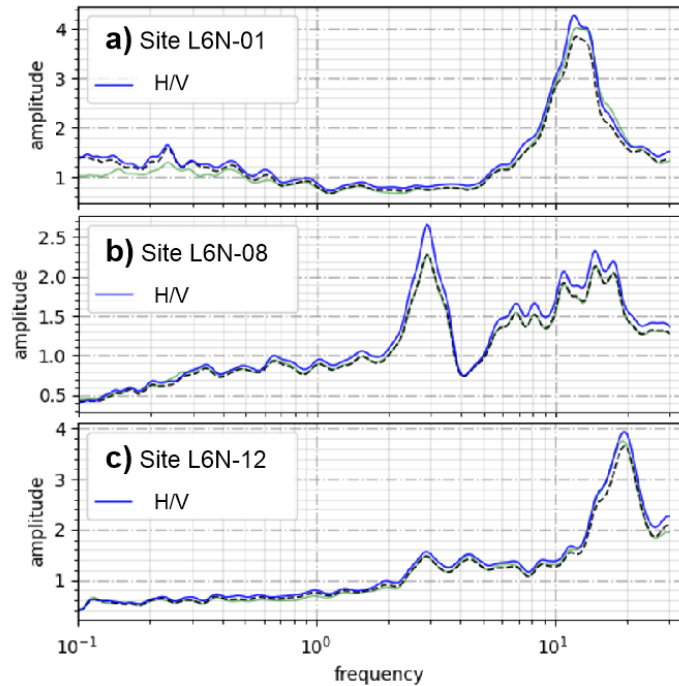


Figure A6. Three examples of H/V spectral ratio curves from sites with a) shallow bedrock; $f_0 = 12.2$ Hz, b) deep bedrock; $f_0 = 2.9$ Hz, and c) a resonating surface layer; $f_1 = 19.7$ Hz and deep bedrock; $f_0 = 2.9$ Hz. Note the varying y-axes.

Information from the S-wave section (Figure A7) confirms that the three HVSR sites presented in Figure A6 are located over a) shallow bedrock (L6N-01), over b) deeper bedrock with shallow layers (L6N-08), and c) over the buried valley with deep layers and a shallow, competent layer (L6N-12). Overlaying of the time-based HVSR curves on the seismic reflection profile supports the interpretation of both datasets in complex settings. For example, an interval of elevated reflection amplitudes combined with the high amplitudes of the HVSR signals is indicative of the bedrock surface (0.05 to 0.08 s) at both ends of Line6N. Both shallow and deep bedrock are well indicated by the HVSR curves usually through the highest amplitude peaks (NW and SE ends of the profile) or local H/V maxima over the buried valley. Deep or dipping bedrock might be obscured by the competent near-surface layer (around 400m distance, SE of site L6N-12). Shallow and intermediate layers can also be observed with HVSR, mainly across the buried valley.

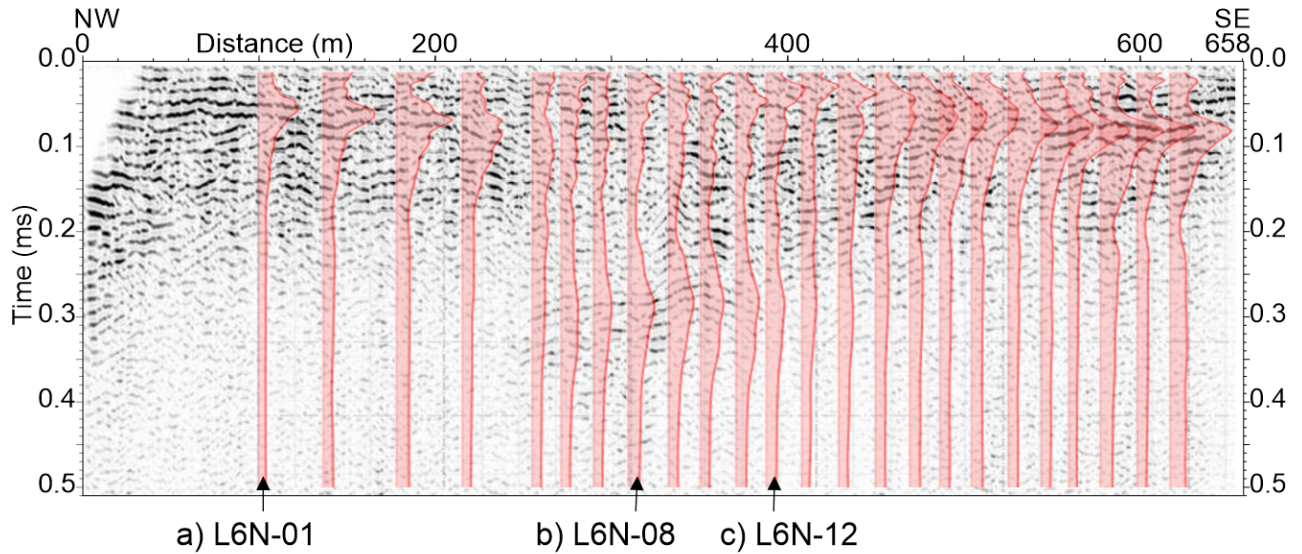


Figure A7. Image of HVSr curves superimposed on seismic profile in two-way travel-time domain. Three HVSr sites presented in Figure A6 are marked.

A1.2.2 DEPTH CONVERSION

Usually, HVSr signals are converted to depth by using a frequency-depth relation that has been calibrated for the region based on HVSr signals obtained at sites with a known subsurface (e.g., core log or geophysically log at a well site; Ibs-von Seht and Wohlenberg, 1999). Since logged wells are sparse in this area, a different approach must be used. Dobry et al. (1976) have developed the analytical solution to the equation of motion of shear waves in uniform (constant density and velocity), horizontal layers as

$$D = V_{s_{av}} / (4F_0) \quad \text{eq. 1}$$

where D is the layer depth, $V_{s_{av}}$ is the average shear-wave velocity and F_0 is the fundamental frequency. Hence, the average shear-wave velocity from the reflection seismic NMO analysis is used as it is in the seismic-reflection depth conversion. An arbitrary adjustment factor of 65% is applied to the velocities to fit the interpreted horizons, as suggested by Dobry et al. (1976) to accommodate velocity gradients rather than uniform layers.

The left side of Figure A8 shows H/V spectral ratios as shaded areas as a function of frequency and distance along the profile with highest amplitude peaks marked with red crosses. The same profile is shown after depth conversion on the right of Figure A8. Notice that the same signal shapes are still visible. Peaks are again marked with red crosses; local maxima are highlighted by blue asterisks making the buried valley and shallow stiff layers more traceable along the profile.

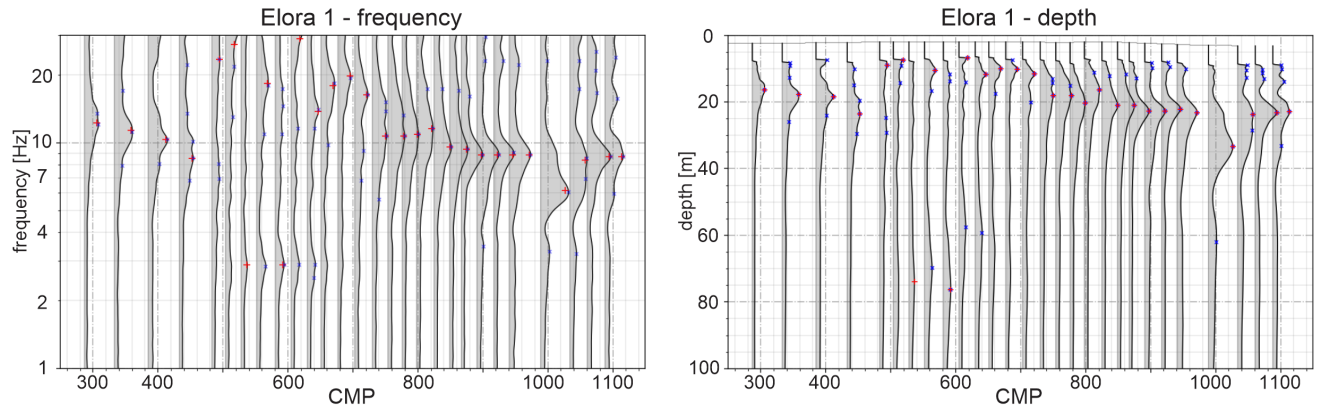


Figure A8. HVSR profile along the Elora 1 – Road6N seismic reflection section referenced to the seismic CMP locations in frequency domain (left) and in depth-domain (right).

Appendix 2: SEISMIC PROFILES IN LARGE FORMAT

Seismic reflection sections are presented as large format PDF files in a special folder in the digital Appendix for all four profile locations. The layout is structured as follows:

- Two columns: S-wave data on the left, P-wave data on the right
- Top row: time-domain sections
- Second row: interpreted depth sections
- Third row: NMO or stacking velocities
- Fourth row: interpretations
- Bottom left: depth-converted H/V amplitudes as green lines, with black lines marking locations
- Bottom right: map indicating profile with CMP numbers

Distance along the profile as well as trace numbers (labelled as CMP – common mid-point) are shown on top of every section. Note that the vertical exaggeration for all depth sections is 1.5x (VE=1.5).

Appendix 3: SEISMIC DATA IN SEG-Y-FORMAT

Seismic reflection profiles are provided in the digital Appendix A3 as seg-y files (seismic standard, Society of Exploration Geophysicists, 2017). Table A3 lists how the provided files are organized into two folders with time-domain and depth-domain data, separated by wave type. The topography is corrected in each file with the reference datum provided in the table. Depth-converted files are organized in the same way, and interval velocity sections are provided in depth domain.

Table A3. List of seismic reflection files contained in the data release for the Guelph – Elora survey.

time-domain		
	P-wave	
		ARB1P340.SGY Arboretum 1, seismic datum = 340 m asl
		ARB2P340.SGY Arboretum 2, seismic datum = 340 m asl
		ELO1P405.SGY Elora 1, seismic datum = 405 m asl
		ELO2P405.SGY Elora 2, seismic datum = 405 m asl
	S-wave	
		ARB1S340.SGY Arboretum 1, seismic datum = 340 m asl
		ARB2S340.SGY Arboretum 2, seismic datum = 340 m asl
		ELO1S405.SGY Elora 1, seismic datum = 405 m asl
		ELO2S405.SGY Elora 2, seismic datum = 405 m asl
depth-domain		
	P-wave	
		Arb1_depth_dp12.sgy Arboretum 1, seismic datum = 340 m asl
		Arb2_depth_dp13.sgy Arboretum 2, seismic datum = 340 m asl
		El1_depth_dp8.sgy Elora 1, seismic datum = 405 m asl
		El2_depth_dp3.sgy Elora 2, seismic datum = 405 m asl
		Arb1_Vpintc_dp12.sgy Arboretum 1, stacking velocity, seismic datum = 405 m asl
		Arb2_Vp_intc_dp13.sgy Arboretum 2, stacking velocity, seismic datum = 405 m asl
		El1_vel_intc_dp8.sgy Elora 1, stacking velocity, seismic datum = 340 m asl
		El2_Vpintc_ds3.sgy Elora 2, stacking velocity, seismic datum = 340 m asl
	S-wave	
		Arb1_depth_ds3.sgy Arboretum 1, seismic datum = 340 m asl
		Arb2_depth_ds5.sgy Arboretum 2, seismic datum = 340 m asl
		El1_depth2_ds18.sgy Elora 1, seismic datum = 405 m asl
		El2_depth_ds2.sgy Elora 2, seismic datum = 405 m asl
		Arb1_Vsintc_ds3.sgy Arboretum 1, stacking velocity, seismic datum = 340 m asl
		Arb2_Vs_intc_ds5.sgy Arboretum 2, stacking velocity, seismic datum = 340 m asl
		El1_Vintc_ds18.sgy Elora 1, stacking velocity, seismic datum = 405 m asl
		El2_VSintc_ds2.sgy Elora 2, sstacking velocity, seismic datum = 405 m asl

Appendix 4: RAW HVSR DATA

Raw Microtremor HVSR data are provided in digital Appendix A4 as mseed files. Each measurement station has its own file with the filename providing station name, UTM coordinates and instrument azimuth. Eastern azimuths (e.g., 8E) need to be subtracted, whereas western azimuths need to be added when correcting (rotating) to true north.